FOXF1 Transcription Factor Is Required for Formation of Embryonic Vasculature by Regulating VEGF Signaling in Endothelial Cells

Xiaomeng Ren, Vladimir Ustiyan, Arun Pradhan, Yuqi Cai, Jamie A. Havrilak, Craig S. Bolte, John M. Shannon, Tanya V. Kalin, Vladimir V. Kalinichenko

Rationale: **Inactivating mutations in the Forkhead Box transcription factor F1 (*FOXF1*) gene locus are frequently found in patients with alveolar capillary dysplasia with misalignment of pulmonary veins, a lethal congenital disorder, which is characterized by severe abnormalities in the respiratory, cardiovascular, and gastrointestinal systems. In mice, haploinsufficiency of the *Foxf1* gene causes alveolar capillary dysplasia and developmental defects in lung, intestinal, and gall bladder morphogenesis.**

Objective: **Although FOXF1 is expressed in multiple mesenchyme-derived cell types, cellular origins and molecular mechanisms of developmental abnormalities in FOXF1-deficient mice and patients with alveolar capillary dysplasia with misalignment of pulmonary veins remain uncharacterized because of lack of mouse models with cell-restricted inactivation of the *Foxf1* gene. In the present study, the role of FOXF1 in endothelial cells was examined using a conditional knockout approach.**

Methods and Results: **A novel mouse line harboring *Foxf1*-floxed alleles was generated by homologous recombination. *Tie2-Cre* and *Pdgfb-CreER* transgenes were used to delete *Foxf1* from endothelial cells. FOXF1-deficient embryos exhibited embryonic lethality, growth retardation, polyhydramnios, cardiac ventricular hypoplasia, and vascular abnormalities in the lung, placenta, yolk sac, and retina. Deletion of FOXF1 from endothelial cells reduced endothelial proliferation, increased apoptosis, inhibited vascular endothelial growth factor signaling, and decreased expression of endothelial genes critical for vascular development, including vascular endothelial growth factor receptors Flt1 and Flk1, Pdgfb, Pecam1, CD34, integrin β3, ephrin B2, Tie2, and the noncoding RNA *Fendrr*. Chromatin immunoprecipitation assay demonstrated that Flt1, Flk1, Pdgfb, Pecam1, and Tie2 genes are direct transcriptional targets of FOXF1.**

Conclusions: **FOXF1 is required for the formation of embryonic vasculature by regulating endothelial genes critical for vascular development and vascular endothelial growth factor signaling. (*Circ Res*. 2014;115:709-720.)**

Key Words: developmental biology ■ endothelial cells ■ pulmonary circulation ■ vascular endothelial growth factor A

Development of the embryonic vasculature depends on vasculogenesis (de novo formation of blood vessels) and angiogenesis (branching of preexisting blood vessels) in a process requiring appropriate levels of vascular endothelial growth factor (VEGF). Targeted disruption of the *Vegf* gene produces an embryonic lethal phenotype displaying impaired blood island formation and delayed endothelial cell differentiation, leading to abnormal blood vessel development.[1,2] VEGF is the ligand for tyrosine kinase receptors Flk1 and Flt1, both of which are expressed in endothelial cells and their mesenchymal precursors. *Flk1*$^{-/-}$ mice die in utero because of inhibition of vasculogenesis and formation of angioblast cells in the blood islands,[3] whereas *Flt1*$^{-/-}$ embryos fail to form mature blood vessels.[4] Other signaling pathways involved in formation of embryonic vasculature include angiopoietin/Tie2, platelet-derived growth factor (PDGF), PI3K/AKT, transforming growth factor-β, Shh, Wnt, and Notch, as well as transcription factors Etv2, Hand1, MEF2c, Prox1, Hey1/2, COUP-TFII, Tbx4, Snail, FOXC2, GATA, Sox, and KLF.[5–7] Identification of additional proteins that regulate embryonic vascular development will provide information regarding pathogenesis of human vascular disorders.

Editorial, see p 683
In This Issue, see p 679

Original received May 14, 2014; revision received July 30, 2014; accepted August 4, 2014. In July 2014, the average time from submission to first decision for all original research papers submitted to *Circulation Research* was 15 days.

From the Divisons of Pulmonary Biology (X.R., V.U., A.P., Y.C., J.A.H., C.S.B., J.M.S., T.V.K., V.V.K.) and Developmental Biology (V.V.K.), Perinatal Institute, Cincinnati Children's Research Foundation, OH.

The online-only Data Supplement is available with this article at http://circres.ahajournals.org/lookup/suppl/doi:10.1161/CIRCRESAHA.115.304382/-/DC1.

Correspondence to Vladimir V. Kalinichenko, MD, PhD, Division of Pulmonary Biology, Cincinnati Children's Research Foundation, 3333 Burnet Ave, MLC 7009, Cincinnati, OH 45229. E-mail Vladimir.Kalinichenko@cchmc.org

Nonstandard Abbreviations and Acronyms	
ACD/MPV	alveolar capillary dysplasia with misalignment of pulmonary veins
ChIP	chromatin immunoprecipitation
ES	embryonic stem
FOXF1	Forkhead Box transcription factor F1
PCR	polymerase chain reaction
PDGF	platelet-derived growth factor
VEGF	vascular endothelial growth factor

Alveolar capillary dysplasia with misalignment of pulmonary veins (ACD/MPV) is a congenital disorder of neonates and infants, which is characterized by severe defects in development of pulmonary capillaries, hypoxemia, pulmonary hypertension and thickening of small pulmonary arteries, malposition of pulmonary veins, lung edema, and impaired lobular development.[8] Structural abnormalities of the genitourinary, gastrointestinal, and cardiovascular systems are also common. Because of the severity of developmental defects and progressive respiratory insufficiency in ACD/MPV infants, the survival after the first month of birth is rare.[8] Although genetic factors associated with ACD/MPV are not fully characterized, heterozygous deletions and point mutations in the Forkhead Box transcription factor F1 (FOXF1) gene locus account for ≈40% of ACD/MPV cases.[9] In addition, genomic deletions in FOXF1 gene were recently found in prenatal cystic hygroma,[10] a congenital vascular defect that can result in fetal hydrops (tissue edema) and embryonic death. These clinical data illustrate a critical role of FOXF1 in vascular development.

FOXF1 protein (previously known as HFH-8 or Freac-1) is a member of the Forkhead Box (Fox) family of transcription factors that share homology in the Winged helix/*Forkhead* DNA–binding domain. FOXF1 is expressed in extraembryonic mesoderm, allantois, splanchnic mesoderm, and septum transversum mesenchyme.[11,12] *Foxf1*$^{-/-}$ mice die by E8.5 because of severe abnormalities in development of the yolk sac and allantois.[13] Although FOXF1 haploinsufficiency causes alveolar capillary dysplasia, fusion of the lung lobes and various developmental defects in mesenchyme of the gallbladder, esophagus, and trachea,[12,14,15] *Foxf1*$^{+/-}$ mice do not recapitulate all histopathologic features of human ACD/MPV. Approximately half of *Foxf1*$^{+/-}$ mice survived past birth,[14] but these mice exhibited severe pulmonary hemorrhage in response to lung injury[16] and abnormal liver regeneration after liver injury.[17]

FOXF1 is activated by the Shh signaling pathway through a direct binding of Gli transcription factors to the *Foxf1* promoter region.[15,18] Deletions of Gli-binding sites were found in the FOXF1 gene locus of ACD/MPV patients.[19] *Shh*$^{-/-}$ mouse embryos exhibit a reduction in *Foxf1* mRNA,[15] implicating Shh/Gli signaling in regulation of *Foxf1* gene expression. FOXF1 induces migration of mesenchymal cells through direct transcriptional activation of *Integrin β3* and *Notch-2* genes.[20,21] Although FOXF1 is expressed in multiple mesenchyme-derived cell types, including fibroblasts, peribronchial smooth muscle, endothelial, and hepatic stellate cells, cellular origins and molecular mechanisms of developmental abnormalities in FOXF1-deficient mice and ACD/MPV patients remain uncharacterized because of the lack of mouse models with cell-restricted inactivation of the *Foxf1* gene. In the present study, we generated mice harboring *Foxf1*-floxed alleles and used *Tie2-Cre* and Pdgfb-CreER transgenes to investigate the role of FOXF1 in endothelial cells. We demonstrated that FOXF1 is critical for formation of embryonic vasculature by stimulating endothelial proliferation and promoting the VEGF, PDGF, and Angpt/Tie2 signaling pathways in endothelial cells through direct transcriptional activation of *Flk1*, *Flt1*, *Pdgfb*, and *Tie2* genes.

Methods

Generation of Foxf1-Floxed Mice and Deletion of FOXF1 From Endothelial Cells

Foxf1-targeting vector contained a LoxP site inserted into the *Foxf1* promoter and PGK-gb2 LoxP/FRT-flanked Neomycin (neo) cassette placed into the first intron (Figure 2A). The PGK promoter–driven herpes simplex virus–thymidine kinase gene was placed outside of the *Foxf1* gene homology region for negative selection of nonhomologous recombination in embryonic stem (ES) cells. The *Foxf1*^{fl}-targeting vector was used for electroporation of mouse ES cells (C57Bl/6x129/SVEV), which were selected for neo (G418) and herpes simplex virus–thymidine kinase resistance (ganciclovir). ES cells with the appropriate *Foxf1*^{fl}-targeted locus were used to generate chimeric mice by injecting *Foxf1*^{fl} ES cells into mouse blastocysts. Mice containing the *Foxf1*^{fl}-targeted allele were determined by polymerase chain reaction (PCR) amplification with primers flanking the LoxP sequence located in the *Foxf1* promoter (P1 and P2) and primers located in the 3′ region of the *Foxf1*^{fl} allele (P3 and P4) (Figure 2A and 2B; and Online Table I). To produce *Foxf1*$^{fl/+}$ mice, chimeric mice were bred with C57Bl/6 mice in the animal facility of Cincinnati Children's Hospital Medical Center. The Neo cassette was deleted by breeding of *Foxf1*$^{fl/+}$ mice with ACT-FLP1 mice (Jackson Laboratory; Figure 2A). The loss of Neo in *Foxf1*$^{fl/+}$ mice was confirmed by PCR using P5 and P6 primers (Figure 2A; Online Table I). *Foxf1*$^{fl/+}$ mice were backcrossed to generate viable *Foxf1*$^{fl/fl}$ mice that were bred into the C57Bl/6 background for 10 generations. Deletion of the *Foxf1*^{fl} alleles from endothelial cell lineage was accomplished through breeding with *Tie2-Cre* (C57Bl/6; Jackson Laboratory) and *Pdgfb-CreER* (C57Bl/6[22]) transgenic mice. To activate *Pdgfb-CreER*, tamoxifen was given in food (200 mg of tamoxifen citrate with 24.8 g sucrose per kilogram of diet; Harlan Laboratory) at E9.5. For postnatal activation of Cre, tamoxifen was injected intraperitoneally (20 μg per day) at postnatal days P0, P1, and P2. Deletion of FOXF1 was confirmed by breeding FOXF1-deficient mice with *LoxP-stop-LoxP-β-gal* (R26R) and *LoxP-tdTomato-LoxP-GFP* (*mT/mG*) reporter mice (both from Jackson Laboratory). *Flk1*-null mutant mice were previously described.[23] Animal studies were approved by the Animal Care and Use Committee of Cincinnati Children's Hospital Research Foundation.

RNA Preparation and Quantitative Real-Time Reverse Transcriptase PCR

Total RNA was prepared from MFLM-91U cells, mouse tissue, and flow-sorted endothelial cells using RNeasy micro kit (Qiagen). Quantitative reverse transcriptase PCR analysis was performed using a StepOnePlus Real-Time PCR system (Applied Biosystems) as described.[24] Samples were amplified using inventoried TaqMan primers (Online Table II). Reactions were analyzed in triplicates, and expression levels were normalized to β-actin mRNA.

Small Interfering RNA Transfection, Western Blot, and Matrigel Angiogenesis Assay

MFLM-91U cells[20] were cultured in serum-free UltraCULTURE medium (Lonza, Walkersville, MD). To inhibit FOXF1, we transfected either nontargeting small interfering RNA or small interfering RNA specific to mouse *Foxf1* (Dharmacon) using Lipofectamine 2000 reagent (Invitrogen) as described.[20,25] Cells were harvested 48

hours after transfection and used for matrigel angiogenesis assay (BD Biosciences). VEGF 165 (20 ng/mL; Millipore) was added to matrigel for 14 hours. Cells in matrigel were stained with calcein AM fluorescent viability dye, which is transported through the cellular membrane into live cells. Confocal 3-dimensional images were quantitated using IMARIS software (Bitplane, CT). Western blot analysis was performed using antibodies described in the Online Data Supplement. Detection of the immune complex was accomplished by using secondary antibodies directly conjugated with horseradish peroxidase followed by the Supersignal chemiluminescence substrate (Pierce, Rockford, IL).

Immunohistochemical Staining and Flow Cytometry

Paraffin sections were stained with H&E or used for immunohistochemical staining as described.[26,27] Primary antibodies and detection systems are listed in the Online Data Supplement. For colocalization experiments, secondary antibodies conjugated with Alexa Fluor 488 or Alexa Fluor 594 (Invitrogen) were used as previously described.[28,29] Slides were counterstained with DAPI (Vector Laboratory). Fluorescent images were obtained using a Zeiss Axioplan2 microscope equipped with an AxioCam MRm digital camera and AxioVision 4.3 Software (Carl Zeiss Microimaging, Thornwood, NY). Flow cytometry was performed using cells isolated from yolk sacs and lungs as described.[27,30] Antibodies used for flow cytometry are listed in the Online Data Supplement. BrdU was injected intraperitoneally into pregnant females 2 hours before embryo harvest. Annexin V kit was from eBioscience. Stained cells were separated using cell sorting (Five-laser FACSAria II; BD Biosciences). Purified cells were used for RNA preparation and quantitative reverse transcriptase PCR analysis.

Chromatin Immunoprecipitation Assay

Chromatin immunoprecipitation (ChIP) assay was performed using in situ cross-linked MFLM-91U cells as described.[24,27] Antibodies used for ChIP were: FOXF1[20] and control rabbit IgG (Vector Laboratory). Sense and antisense PCR primers that were used to amplify mouse promoter DNA fragments in ChIP assay are provided in Online Table III.

Statistical Analysis

ANOVA and Student *t* test were used to determine statistical significance. *P* values <0.05 were considered significant. Values for all measurements were expressed as the mean±SD.

Results

FOXF1 Is Expressed in Mesenchyme and Endothelial Cells During Embryogenesis

Immunostaining with FOXF1 antibodies was used to visualize FOXF1-expressing cells in E13.5 mouse embryos. FOXF1 protein was found in mesenchyme of the lung, trachea, esophagus, stomach, intestine, oral cavity, tongue, and cartilage (Figure 1A–1I), which is consistent with previous in situ hybridization studies.[11,13] Additional site of FOXF1 expression was found in the embryonic heart where FOXF1 was present in mesenchyme of cardiac cushion but absent from myocardium and endocardial cells (Figure 1E; data not shown). FOXF1 was detected in hemangioblasts of the yolk sac but was absent from hematopoietic cells at E8.5 to E12.5 (Figure 1O; data not shown). FOXF1 was also detected in nuclei of endothelial cells of the lung, yolk sac, and embryonic regions of the placenta (Figure 1J–1N). FOXF1 protein colocalized with endothelial marker proteins Flk1, Isolectin B4, and Von Willebrand factor in lung tissue (Figure 1P–1R). Thus, FOXF1 is expressed in endothelial cells during embryogenesis.

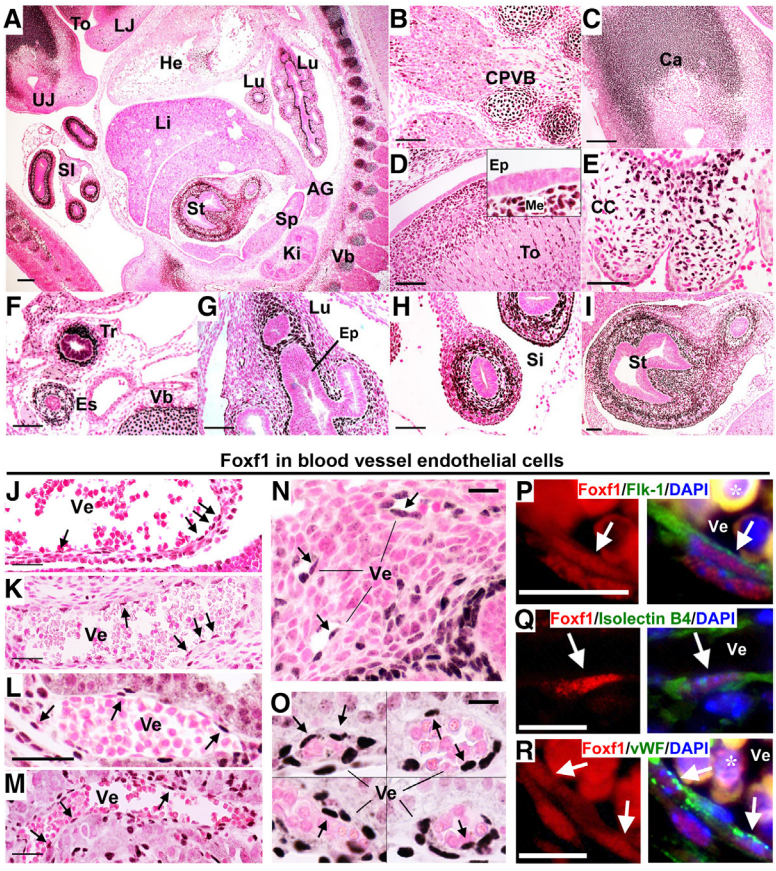

Figure 1. Forkhead Box transcription factor F1 (FOXF1) is expressed in mesenchymal and endothelial cells of the developing embryo. A to **I**, Immunostaining shows that FOXF1 is expressed in mesenchyme-derived cells in E13.5 wild-type mouse embryos (**A**). FOXF1 is detected in cartilage primordiums of vertebral bodies (CPVB in **B**), oral cavity (Ca in **C**), tongue (To in **D**), atrioventricular cardiac cushions (CC in **E**), trachea (Tr), and esophagus (Es in **F**), lung (Lu in **G**), small intestine (Si in **H**), stomach (St in **I**). **J** to **O**, FOXF1 is expressed in endothelial cells. Low levels of FOXF1 were detected in a subset of endothelial cells (shown with arrows) located in the inferior vena cava (**J**) and pulmonary vein (**K**). FOXF1 is detected in blood vessels of the yolk sac (**L** and **O**), lung (**N**), and the fetal part of the placenta (**M**). A composite of 4 different images is shown in **O**. FOXF1 protein was not found in hematopoietic cells. **P** to **R**, FOXF1 colocalizes with endothelial markers Flk1 (**P**), Isolectin B4 (**Q**), and Von Willebrand factor (**R**) in E12.5 lungs. Location of FOXF1 in nuclei of endothelial cells is shown with white arrows. Autofluorescence of red blood cells is denoted with *. AG indicates adrenal gland; ep, epithelial cells; He, heart; Ki, kidney; Li, liver; LJ, lower jaw; me, mesenchyme; Sp, spleen; UJ, upper jaw; Vb, vertebrae; and Ve, blood vessel. Scale bars, 100 μm (**A**), 50 μm (**B**–**M**), 20 μm (**N**–**O**), and 10 μm (**P**–**R**).

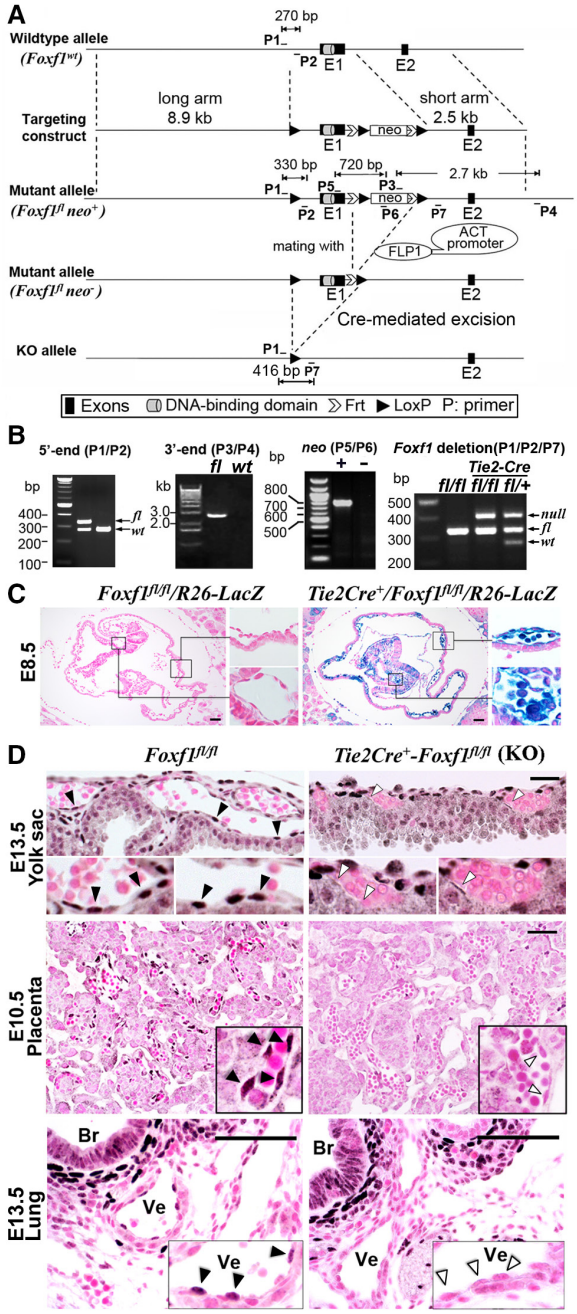

Figure 2. Generation of *Foxf1*$^{fl/fl}$ mice and conditional deletion of Forkhead Box transcription factor F1 (FOXF1) from endothelial cells. A, Schematic diagram of *Foxf1* gene-targeting construct with 2 *Frt* sites (white arrows) and 3 *LoxP* sites (black arrowheads) that surround the Neomycin (neo) gene and exon 1 (E1), encoding the DNA-binding domain of the FOXF1 protein. The Neo cassette was removed after breeding of *Foxf1-floxed* mice with β-actin (ACT)–FLP1 mice. Endothelial deletion of FOXF1 was achieved by breeding with *Tie2-Cre* mice. **B**, Polymerase chain reaction of mouse tail DNA using primers (P1–P7). Locations of primers are indicated in **A**. **C**, β-gal activity (blue staining) is detected in both endothelial and hematopoietic cells in the yolk sac of *Tie2-Cre Foxf1*$^{fl/+}$*/R26R* E8.5 embryos. Slides were counterstained with nuclear fast red (red nuclei). Inserts show blood vessels in the yolk sac (**top**) and embryo proper (**bottom**). **D**, Immunostaining shows the presence of FOXF1 protein in endothelial cells (black arrowheads) of control *Foxf1*$^{fl/fl}$ embryos. FOXF1 staining is absent from majority of endothelial cells of *Tie2-Cre Foxf1*$^{fl/fl}$ embryos (white arrowheads). Br indicates bronchiole; and Ve, blood vessel. Scale bars, 50 μm.

Table. Genotype Frequency of Offspring From the Breeding of *Tie2-Cre*$^{+/-}$*Foxf1*$^{fl/wt}$ Males and *Foxf1*$^{fl/fl}$ Females

	Total Embryos	*Foxf1*$^{fl/wt}$	*Foxf1*$^{fl/fl}$	*Tie2-Cre*$^{+/-}$ *Foxf1*$^{fl/wt}$	*Tie2-Cre*$^{+/-}$ *Foxf1*$^{fl/fl}$
Theoretical ratio		25%	25%	25%	25%
Experimental ratio					
E10.5	55	14 (25%)	15 (27%)	14 (25%)	13 (24%)
E11.5	39	14 (36%)	8 (21%)	7 (18%)	10 (26%)
E12.5	60	20 (33%)	9 (15%)	12 (20%)	19 (32%)
E13.5	74	21 (28%)	20 (27%)	20 (27%)	13 (18%)*
E14.5	21	6 (29%)	7 (33%)	6 (29%)	2 (10%)*
E15.5–16.5	17	2 (12%)	7 (41%)	7 (41%)	1 (6%)*

*Significant differences between experimental and theoretical ratios.

Generation of Foxf1-Floxed Mice and Deletion of Foxf1 From Endothelial Cells

Given the importance of FOXF1 in pathogenesis of ACD/MPV in humans, we determined FOXF1 requirements in endothelial cells using a conditional knockout approach. A triple-LoxP *Foxf1-floxed* targeting vector containing the Neo cassette and 2 *Frt* sites was constructed (Figure 2A) and used for electroporation of mouse ES cells. After mouse blastocyst injection of the Neo-resistant *Foxf1*$^{fl/+}$ ES cells, chimeric mice with germline transmission were obtained and bred to generate a stable *Foxf1*$^{fl/+}$ mouse line. The Neo cassette was deleted by breeding *Foxf1*$^{fl/+}$ mice with ACT-FLP1 mice (Figure 2A). PCR amplification of mouse tail genomic DNA was used to distinguish between *Foxf1-floxed* and *Foxf1-wild type* (wt) alleles (Figure 2B). The *Foxf1*$^{fl/fl}$ mice were bred with *Tie2-Cre* mice to delete the first exon of the *Foxf1* gene encoding the DNA-binding domain and part of the transcriptional activation domain of the FOXF1 protein (Figure 2A; Online Figure I), both of which are required for FOXF1 transcriptional activity.[9,21] Cre-mediated recombination and the loss of FOXF1 protein in *Tie2-Cre Foxf1*$^{fl/fl}$ endothelial cells were confirmed by *Rosa26-LacZ* reporter (Figure 2C) and immunostaining with FOXF1 antibodies (Figure 2D).

Embryonic Lethality and Cardiovascular Defects in *Tie2-Cre Foxf1*$^{fl/fl}$ Embryos

Tie2-Cre Foxf1$^{fl/fl}$ embryos were present in Mendelian ratio before E13.5 (Table). The number of *Tie2-Cre Foxf1*$^{fl/fl}$ embryos progressively decreased from E13.5 to E16.5, consistent with embryonic lethality during this period (Table). Histological examination of the *Tie2-Cre Foxf1*$^{fl/fl}$ embryos revealed severe growth retardation as demonstrated by decreased embryo size and body weight (Figure 3A). Liver size was also decreased in FOXF1 mutants (Figure 3B). Deletion of FOXF1 caused ventricular hypoplasia and an interventricular septal defect in the embryonic heart (Online Figure IIA and IIB). Furthermore, FOXF1 mutants exhibited accumulation of fluid in the amniotic cavity (polyhydramnios) and pericardial cavity (pericardial efflux; Figure 3A), a common finding in embryos with various cardiovascular abnormalities.[5,6] Thus, deletion of FOXF1 resulted in embryonic lethality because of severe growth retardation and cardiovascular defects.

FOXF1 Deletion Impairs the Formation of Embryonic Vasculature in the Yolk Sac and Placenta

At E13.5, vascular branching was reduced in the yolk sac and placenta of *Tie2-Cre Foxf1*$^{fl/fl}$ embryos when compared with control *Foxf1*$^{fl/fl}$ embryos (Figure 3C; Online Figure IIIA). Reduced vascular branching was confirmed by whole-mount immunostaining of yolk sacs for endothelial-specific endomucin (Figure 3D). Decreased vascular branching and polyhydramnios were also found in the yolk sac of *Foxf1*$^{+/-}$ embryos (Online Figure IIIB and IIIC), findings consistent with published studies.[14,15] Vascular phenotypes in *Tie2-Cre Foxf1*$^{fl/fl}$ and *Foxf1*$^{+/-}$ embryos were less severe compared with *Flk1*-null mutant mice that exhibited growth retardation, a near-complete loss of yolk sac vasculature and embryonic lethality at E10.5 (Online Figure IIID).

Vascular defects in *Tie2-Cre Foxf1*$^{fl/fl}$ yolk sacs were associated with reduced *Foxf1* mRNA (Figure 4A) and decreased expression of *Flt1*, *Flk1*, and *angiopoietin-1* (Figure 4B), all of which are critical for angiogenesis and VEGF signaling in endothelial cells.[3,4,23,31] *Angpt2* and *Nrp*1 mRNAs were increased in FOXF1 mutants (Figure 4B). Expression of Ephrin B2 was reduced in arteries of *Tie2-Cre Foxf1*$^{fl/fl}$ embryos (Online Figure IVA) as well as in isolated Pecam1^{+} endothelial cells

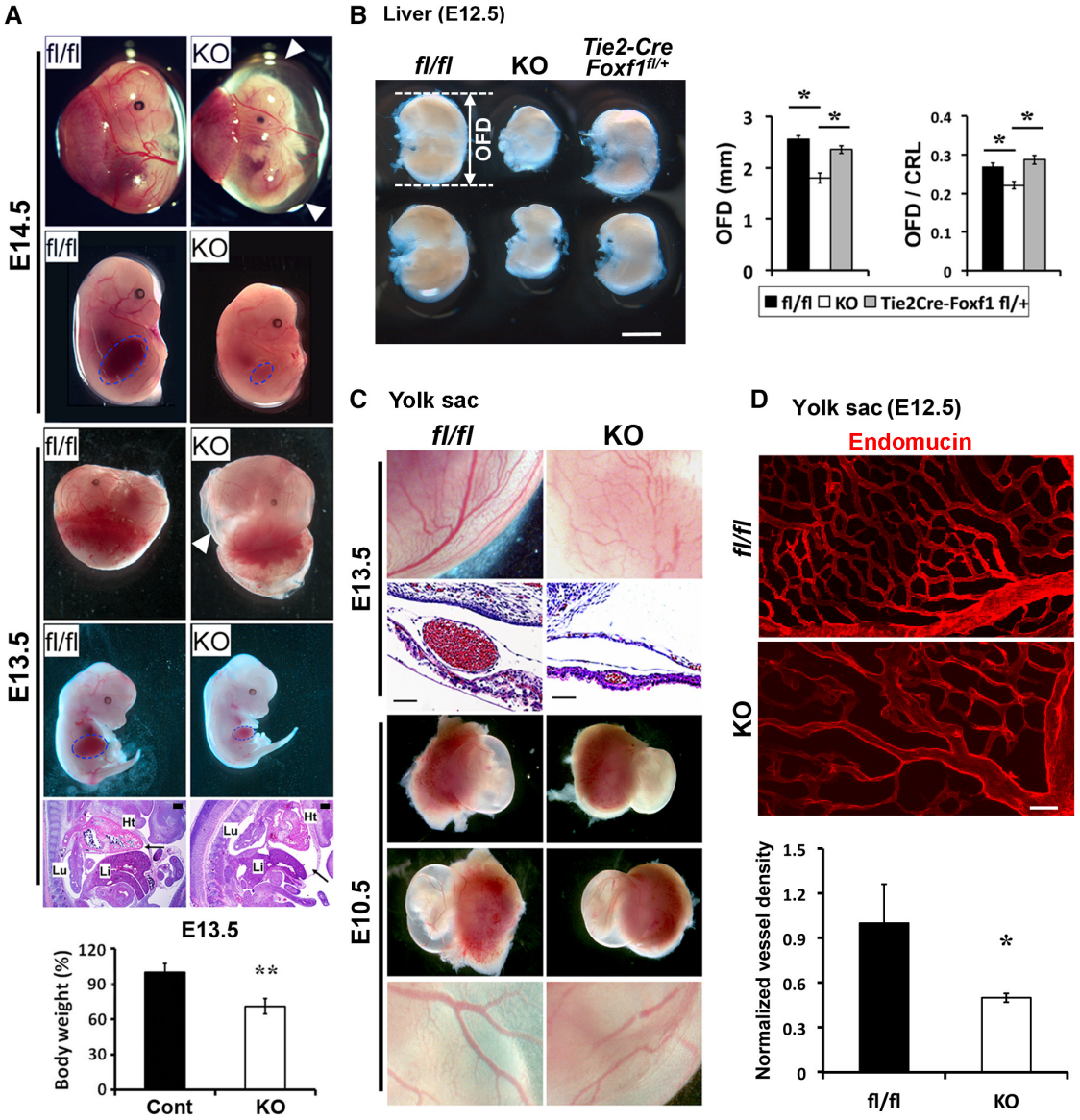

Figure 3. Embryonic abnormalities in *Tie2-Cre Foxf1*$^{fl/fl}$ embryos. A, *Tie2-Cre Foxf1*$^{fl/fl}$ embryos (knockout) exhibit growth retardation and severe polyhydramnios (white arrowheads) at E13.5 to 14.5. *Foxf1*$^{fl/fl}$ littermates (fl/fl) are shown for comparison. Boundary of the liver is indicated by blue line. Pericardial efflux is shown with a black arrow on H&E-stained section of *Tie2-Cre Foxf1*$^{fl/fl}$ embryos. Body weight is decreased in *Tie2-Cre Foxf1*$^{fl/fl}$ E13.5 embryos (n=10) compared with control *Foxf1*$^{fl/fl}$ littermates (n=43). **B**, Liver size was decreased in *Tie2-Cre Foxf1*$^{fl/fl}$ embryos. Occipital frontal diameter (OFD) of the liver and the ratio between OFD and the crown rump length (CRL) were significantly reduced after deletion of Forkhead Box transcription factor F1 (FOXF1; n=5). **C** and **D**, Diminished vascular branching in the yolk sac of FOXF1-deficient embryos. The whole-mount immunoistaining was performed using endomucin Abs. Confocal microscopy was used to quantify the vessel density as a ratio between endothelial (endomucin) and epithelial (E-cadherin) staining (**bottom**; **D**). *P<0.05, **P<0.01. Ht indicates, heart; Li, liver; and Lu, lung. Scale bars, 50 μm (**A**), 1 mm (**B**), 50 μm (**C**), and 100 μm (**D**).

(Online Figure IVB). There were no differences in the number of lymphatic vessels stained for LYVE1 (Online Figure IVA). *Ephrin b4*, *Sox-18*, *Foxc1*, and *Foxc2* mRNAs were unaltered (Online Figure IVB and IVC). Interestingly, when the *Tie2-Cre Foxf1$^{fl/fl}$* embryos were examined at E10.5, diminished branching of blood vessels was still evident in the yolk sac and placenta (Figure 3C; data not shown), but cardiac abnormalities and polyhydramnios were absent (Figure 3C; Online Figure IIC). The number of Pecam1^{+}/ Tie2^{+}/ CD45^{-} endothelial cells was reduced in *Tie2-Cre Foxf1$^{fl/fl}$* E10.5 yolk sacs (Online Figure VB), whereas the number of Pecam1^{-}/ CD45^{+} and Pecam^{-}/ CD41^{+} hematopoietic cells was normal (Online Figure VA). Thus, vascular insufficiency in the yolk sac and placenta occurs earlier than other embryonic defects and is likely to be a primary cause of growth retardation and embryonic lethality in *Tie2-Cre Foxf1$^{fl/fl}$* embryos. Altogether, FOXF1 deletion from endothelial cells impairs heart development and decreases vascular branching in the yolk sac and placenta.

FOXF1 Deletion Impairs the Formation of Pulmonary Vascular Plexus

Because FOXF1 deficiency is associated with reduced numbers of pulmonary capillaries in ACD/MPV infants and *Foxf1$^{+/-}$* embryos,[8,14] we examined vasculature in *Tie2-Cre Foxf1$^{fl/fl}$* lungs. Similar to the yolk sac and placenta, diminished number of blood vessels was observed in the lung of *Tie2-Cre Foxf1$^{fl/fl}$* embryos, as demonstrated by reduced staining for endothelial-specific markers PECAM-1 and SOX-17 (Figure 4C). Despite impaired vasculature, epithelial tubules were still present in *Tie2-Cre Foxf1$^{fl/fl}$* lungs (Figure 4C). Flk1 staining and *Flk1* mRNA were reduced after deletion of FOXF1 (Figure 4C and 4D). *Flt1*, *Pecam-1*, *Sox-17*, *CD34*, and *Pdgfb* mRNAs were decreased in whole-lung RNA from *Tie2-Cre Foxf1$^{fl/fl}$* embryos (Figure 4D), confirming the loss of pulmonary vascular plexuses.

Reduced Vascular Branching in *Pdgfb-CreER Foxf1$^{fl/fl}$* Embryos

Pdgfb-CreER Foxf1$^{fl/fl}$ mouse line was generated to achieve an inducible deletion of *Foxf1* from endothelial cells without targeting hematopoietic cells. To activate Cre, tamoxifen was given to pregnant females at E9.5, and embryos were harvested at E12.5. The *Foxf1*-null allele was detected in tamoxifen-treated *Pdgfb-CreER Foxf1$^{fl/fl}$* mice by PCR (Figure 5A), a finding consistent with activation of Cre by tamoxifen. Cre-mediated recombination in lung tissue was confirmed by β-gal reporter and diminished FOXF1 immunostaining (Figure 5B). Flow cytometry showed that ≈60% of PECAM-1^{+} endothelial cells and only 2% of CD45^{+} hematopoietic cells in the yolk sac were positive for Cre (Figure 5A). *Pdgfb-CreER Foxf1$^{fl/fl}$* embryos exhibited polyhydramnios (Figure 5A), reduced vascular branching in the placenta and yolk sac (Figure 5C), and decreased numbers of endothelial cells in the lung (Figure 5D). Deletion of FOXF1 during the postnatal period (P0–P2) impaired retinal angiogenesis in *Pdgfb-CreER Foxf1$^{fl/fl}$* mice (Online Figure VI). Thus, FOXF1 stimulates angiogenesis in the developing lung, eye, placenta, and yolk sac.

FOXF1 Stimulates Angiogenesis In Vitro

The ability of FOXF1 to stimulate angiogenesis in endothelial cells was directly tested in vitro. Small interfering RNA transfection was used to deplete FOXF1 mRNA and protein in endothelial MFLM-91U cells (Figure 6B and 6C). Depletion of FOXF1 reduced the ability of MFLM-91U cells to form vessel-like sprouts in matrigel (Figure 6A), a common model of angiogenesis in vitro. Diminished angiogenesis in FOXF1-depleted cells was associated with reduced proteins and mRNAs of *Flk1*, *Flt1*, *Pecam-1*, and *Pdgfb*, whereas

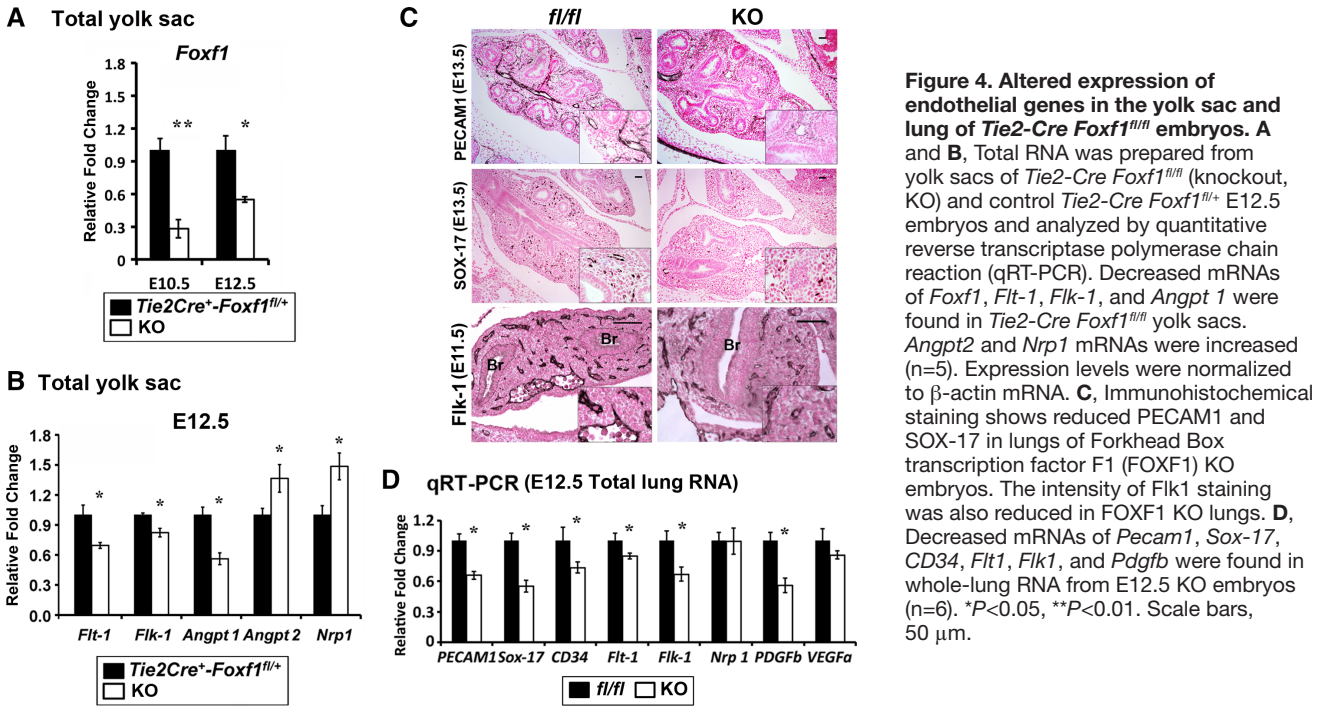

Figure 4. Altered expression of endothelial genes in the yolk sac and lung of *Tie2-Cre Foxf1$^{fl/fl}$* embryos. A and **B**, Total RNA was prepared from yolk sacs of *Tie2-Cre Foxf1$^{fl/fl}$* (knockout, KO) and control *Tie2-Cre Foxf1$^{fl/+}$* E12.5 embryos and analyzed by quantitative reverse transcriptase polymerase chain reaction (qRT-PCR). Decreased mRNAs of *Foxf1*, *Flt-1*, *Flk-1*, and *Angpt 1* were found in *Tie2-Cre Foxf1$^{fl/fl}$* yolk sacs. *Angpt2* and *Nrp1* mRNAs were increased (n=5). Expression levels were normalized to β-actin mRNA. **C**, Immunohistochemical staining shows reduced PECAM1 and SOX-17 in lungs of Forkhead Box transcription factor F1 (FOXF1) KO embryos. The intensity of Flk1 staining was also reduced in FOXF1 KO lungs. **D**, Decreased mRNAs of *Pecam1*, *Sox-17*, *CD34*, *Flt1*, *Flk1*, and *Pdgfb* were found in whole-lung RNA from E12.5 KO embryos (n=6). *P<0.05, **P<0.01. Scale bars, 50 μm.

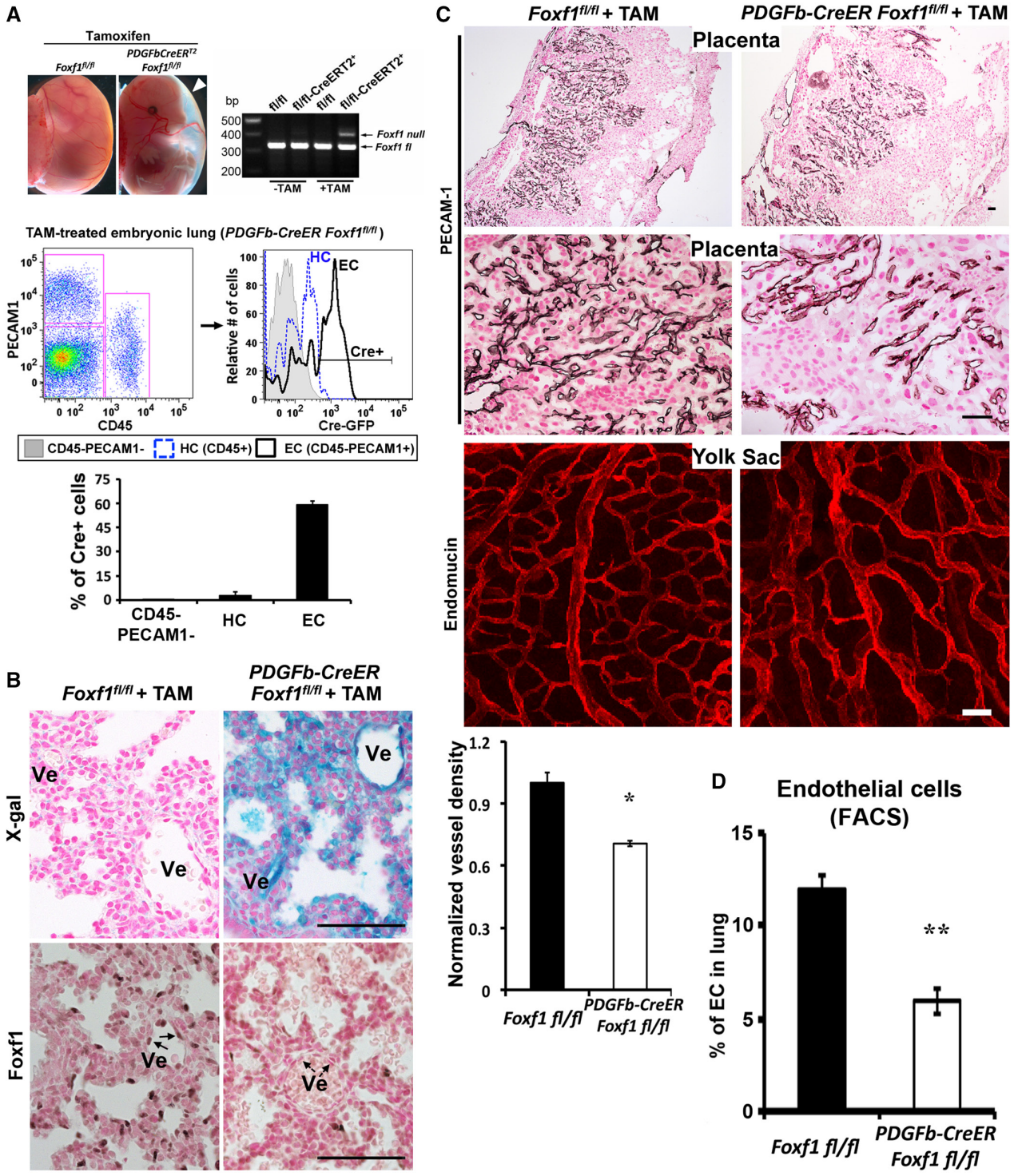

Figure 5. Reduced vascular branching in *Pdgfb-CreER Foxf1*$^{fl/fl}$ embryos. A, *Pdgfb-CreER Foxf1*$^{fl/fl}$ embryos were treated with tamoxifen at E9.5 and harvested at E12.5. Polyhydramnios in Forkhead Box transcription factor F1 (FOXF1)–deficient embryos is indicated with white arrowhead. Polymerase chain reaction of genomic tail DNA shows Cre-mediated recombination. Flow cytometry shows GFP fluorescence, which is associated with the *Pdgfb-CreER* transgene, in 60% of Pecam1$^+$ endothelial cells (ECs) isolated from the yolk sac. GFP is not detected in a majority of CD45$^+$ hematopoietic cells (HCs). **B**, Increased β-gal activity and decreased FOXF1 staining is observed in lungs of *Pdgfb-CreER Foxf1*$^{fl/fl}$*/R26R* E17.5 embryos. **C**, Immunostaining for Pecam1 and endomucin shows reduced vessel (Ve) density in the placenta and yolk sac of FOXF1-deficient embryos. Quantification is shown in **bottom**. **D**, Decreased numbers of Pecam1$^+$ endothelial cells are found in FOXF1-deficient lungs by flow cytometry (n=5). *P<0.05, **P<0.01. Scale bars, 50 μm.

expression of *Angpt2* was increased (Figure 6B and 6C). After depletion of FOXF1, phosphorylation of ERK and AKT was decreased (Figure 6D), indicating reduced VEGF signaling. Interestingly, VEGF-A ligand did not rescue the FOXF1-mediated decrease in angiogenesis (Figure 6A and 6D), a finding consistent with reduced expression of VEGF receptors in

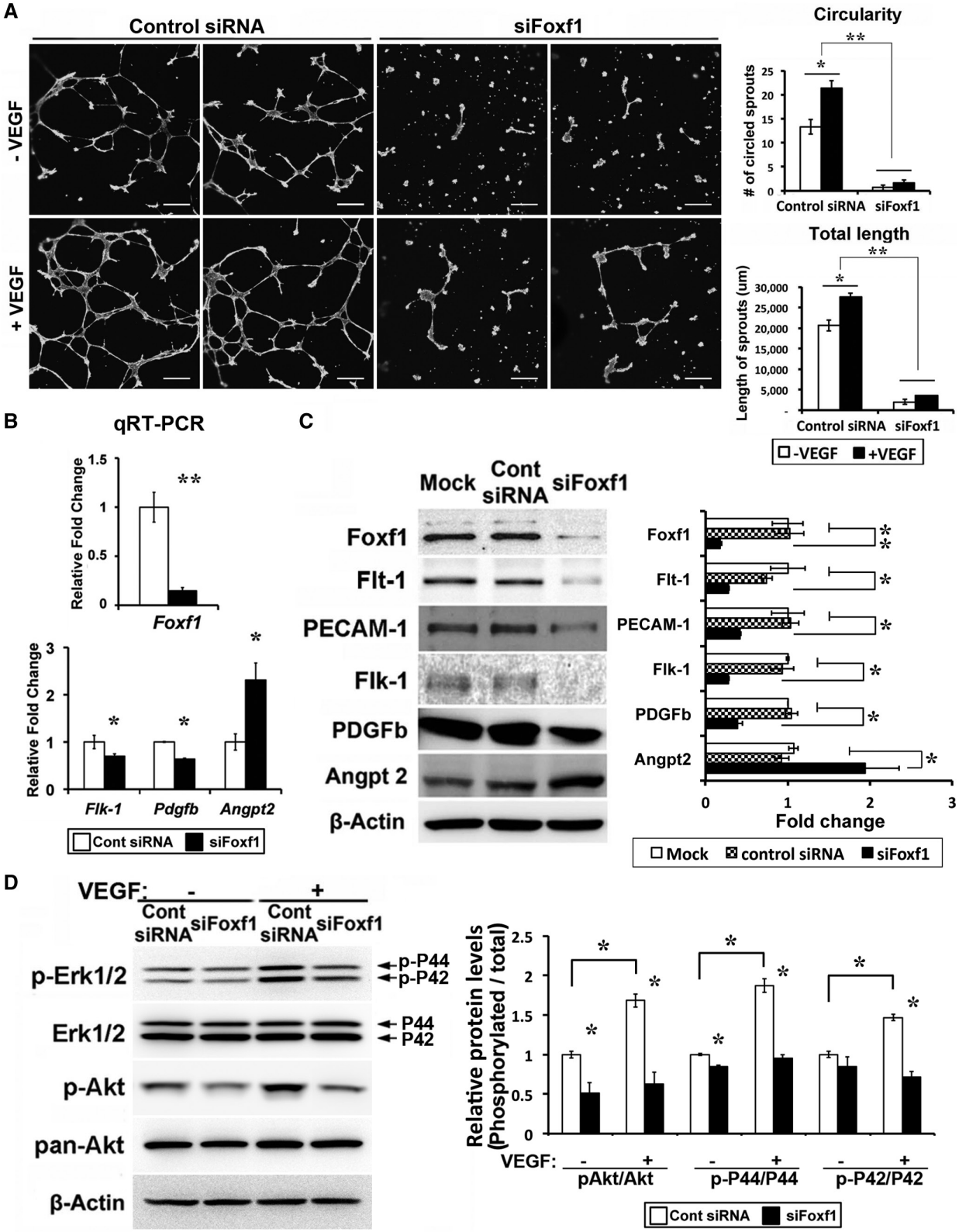

Figure 6. Small interfering RNA (siRNA)–mediated depletion of Forkhead Box transcription factor F1 (FOXF1) impairs angiogenesis in matrigel and inhibits vascular endothelial growth factor (VEGF) signaling in cultured MFLM-91U cells. A, MFLM-91U cells were transfected with either FOXF1 siRNA or control nontargeting siRNA. Forty-eight hours after siRNA transfection, matrigel angiogenesis assay was performed in the presence and absence of VEGF-A(165). FOXF1 knockdown reduced the number and total length of endothelial sprouts (n=5). **B**, Quantitative reverse transcriptase polymerase chain reaction (qRT-PCR) shows reduced *Foxf1*, *Flk1*, and *Pdgfb* mRNAs at 24 h after siRNA transfection. *Angp2* mRNA was increased after depletion of FOXF1. **C**, Altered protein levels of FOXF1, Flk1, Flt1, PECAM-1, PDGFb, and Angpt2 at 48 h after siRNA transfection are shown by Western blots. **D**, FOXF1-depleted MFLM-91U cells are resistant to VEGF-A(165) stimulation as indicated by decreases in phosphorylated Erk1/2 (pErk1/2) and phosphorylated Akt (pAkt). Quantification of Western blots is shown in right panels in **C** and **D**. **P*<0.05, ***P*<0.01. Scale bars, 500 μm.

FOXF1-depleted cells. Thus, FOXF1 promotes VEGF signaling and increases angiogenesis in vitro.

Decreased Proliferation and Increased Apoptosis in Endothelial Cells of *Tie2-Cre Foxf1$^{fl/fl}$* Embryos

VEGF induces cellular proliferation and inhibits apoptosis by activating the tyrosine kinase receptor Flk1, which is present on the surface of endothelial cells.[3,6] Given that Flk1 mRNA and protein were decreased in FOXF1-deficient mice (Figure 4B–4D) and cultured MFLM-91U cells (Figure 6B and 6C), we next determined whether FOXF1 affects endothelial proliferation and apoptosis in vivo. Yolk sacs from E12.5 embryos were enzymatically digested and cells were stained for the endothelial marker Pecam-1 and the hematopoietic marker CD45 followed by flow cytometry. Consistent with reduced VEGF/ Flk1 signaling, DNA replication was decreased in Pecam-1$^+$/ CD45$^-$ endothelial cells of *Tie2-Cre Foxf1$^{fl/fl}$* yolk sacs as demonstrated by reduced BrdU incorporation into DNA (Figure 7A). In addition, apoptosis of FOXF1-deficient endothelial cells was increased as shown by annexin V staining (Figure 7A). Thus, reduced proliferation and increased apoptosis of endothelial cells can contribute to reduced angiogenesis and embryonic lethality in *Tie2-Cre Foxf1$^{fl/fl}$* mice.

FOXF1 Directly Regulates Expression of Endothelial Genes Critical for Angiogenesis and VEGF Signaling

To label endothelial cells that underwent Cre-mediated recombination, *Tie2-Cre Foxf1$^{fl/+}$* mice were crossed with *mT/mG* reporter mice that contain the *LoxP-tdTomato-LoxP-GFP* cassette knocked into the *Rosa26* locus. The use of *mTmG* reporter enabled us to distinguish between Cre-targeted (GFP$^+$) and nontargeted (tdTomato$^+$) endothelial cells in *Tie2-Cre Foxf1$^{fl/fl}$/mT/mG* embryos. In control *Foxf1$^{fl/fl}$/mTmG* embryos, both endothelial (Pecam-1$^+$/ CD45$^-$) and hematopoietic cells (Pecam-1$^{-/-}$CD45$^+$) were negative for GFP but positive for *tdTomato* reporter, indicating the lack of Cre-mediated recombination (Figure 7B). In contrast, 84.1±0.5% of endothelial cells and 71.6±4.6% of hematopoietic cells from *Tie2-Cre Foxf1$^{fl/fl}$/mTmG* embryos were positive for GFP (Figure 7B). We next used flow cytometry–based cell sorting to isolate GFP$^+$ and tdTomato$^+$ endothelial cells and use these cells for quantitative reverse transcriptase PCR. Loss of *Foxf1* mRNA and decreased expression of the FOXF1 target gene, integrin β3,[20] were specifically found in GFP$^+$ endothelial cells compared with control tdTomato$^+$ endothelial cells (Figure 7C). Deletion of FOXF1 efficiently reduced mRNAs of *Flk1*, *Flt1*, *Pdgfb*, *Pecam-1*, *CD34*, *Tie2*, and the noncoding RNA *Fendrr*, all of which are critical for embryonic vascular development.[5–7,32,33] In contrast, *Angpt2*, *Nrp1, Dll4, Notch2*, and *VEGFb* mRNAs were increased (Figure 7C). There was no difference in expression levels of Notch1 and Notch target genes Hey2 and Hes1 (Figure 7C). Finally, ChIP assay demonstrated that FOXF1 protein directly bound to promoter DNAs of *Flk1*, *Flt1*, *Pdgfb*, *Pecam-1*, and *Tie2* (Figure 7D), a finding consistent with a direct transcriptional regulation of these genes by FOXF1. FOXF1 protein did not bind to *Nrp1* and *Angpt2* promoters (Figure 7D). Thus, FOXF1 directly regulates expression of endothelial genes critical for angiogenesis and VEGF signaling.

Discussion

Although various vascular abnormalities were previously reported for *Foxf1$^{-/-}$* and *Foxf1$^{+/-}$* mouse embryos as well as for ACD/MPV infants with FOXF1 mutations,[9,13,14] cellular origins and molecular mechanisms of these developmental defects remain uncharacterized. In the present study, we showed that FOXF1 is expressed in endothelial cells and that endothelial deletion of FOXF1 causes a variety of developmental defects, including impaired vasculature in the yolk sac, placenta, lung, and retina. These data demonstrate that FOXF1 functions in a cell-autonomous manner to induce the formation of embryonic vasculature. This hypothesis is consistent with diminished angiogenesis in FOXF1-deficient endothelial MFLM-91U cells in vitro. Interestingly, during embryogenesis FOXF1 is abundantly expressed in endothelial cells of capillaries and small blood vessels of the yolk sac, placenta, and lung, but found only in a subset of endothelial cells of vena cava and pulmonary vein. In adult mice, FOXF1 was absent from endothelium of large pulmonary vessels but present in pulmonary capillaries.[34] Therefore, FOXF1 is not a marker of endothelial cells. It is possible that FOXF1 expression in endothelial cells depends on proliferation or differentiation status, or reflects endothelial responses to various stimuli.

Although *Tie2-Cre Foxf1$^{fl/fl}$* mutant mice exhibited a complex developmental phenotype, we think that vascular insufficiency in the yolk sac and placenta was a primary cause of growth retardation and embryonic lethality in *Tie2-Cre Foxf1$^{fl/fl}$* embryos. This conclusion is based on the fact that diminished branching of blood vessels was found at E10.5, whereas other developmental abnormalities such as cardiac defects and polyhydramnios occurred after E13.5. Vascular insufficiency in the yolk sac and placenta may alter embryonic circulation in FOXF1 mutants, causing secondary heart defects and polyhydramnios and contributing to embryonic death. Interestingly, FOXF1 is expressed in the cardiac cushion and important for mesenchyme migration[20] (and this article). Therefore, interventricular septal defect in *Tie2-Cre Foxf1$^{fl/fl}$* embryos can be a direct consequence of FOXF1 deletion from mesenchymal cells of cardiac cushion, which is critical for formation of interventricular septum and cardiac valves. FOXF1 was not detected in hematopoietic cells that are targeted by the *Tie2-Cre* transgene in our mouse model, and therefore, it is unlikely that FOXF1 deletion in hematopoietic cell lineages contributed to the vascular phenotype in FOXF1 mutant mice. However, we cannot exclude the possibility that FOXF1 is expressed in rare population(s) of hematopoietic progenitors, and targeting these cells contributed to the phenotype in *Tie2-Cre Foxf1$^{fl/fl}$* embryos. Interestingly, the *Pdgfb-CreER* transgene, which is more specific to endothelial cells compared with the Tie2-Cre,[22] caused similar defects in vascular development, suggesting that endothelial cells are the main cellular targets of FOXF1. It is also possible that FOXF1 deletion reduces the number of circulating endothelial progenitors or mesenchymal stem cells, contributing to

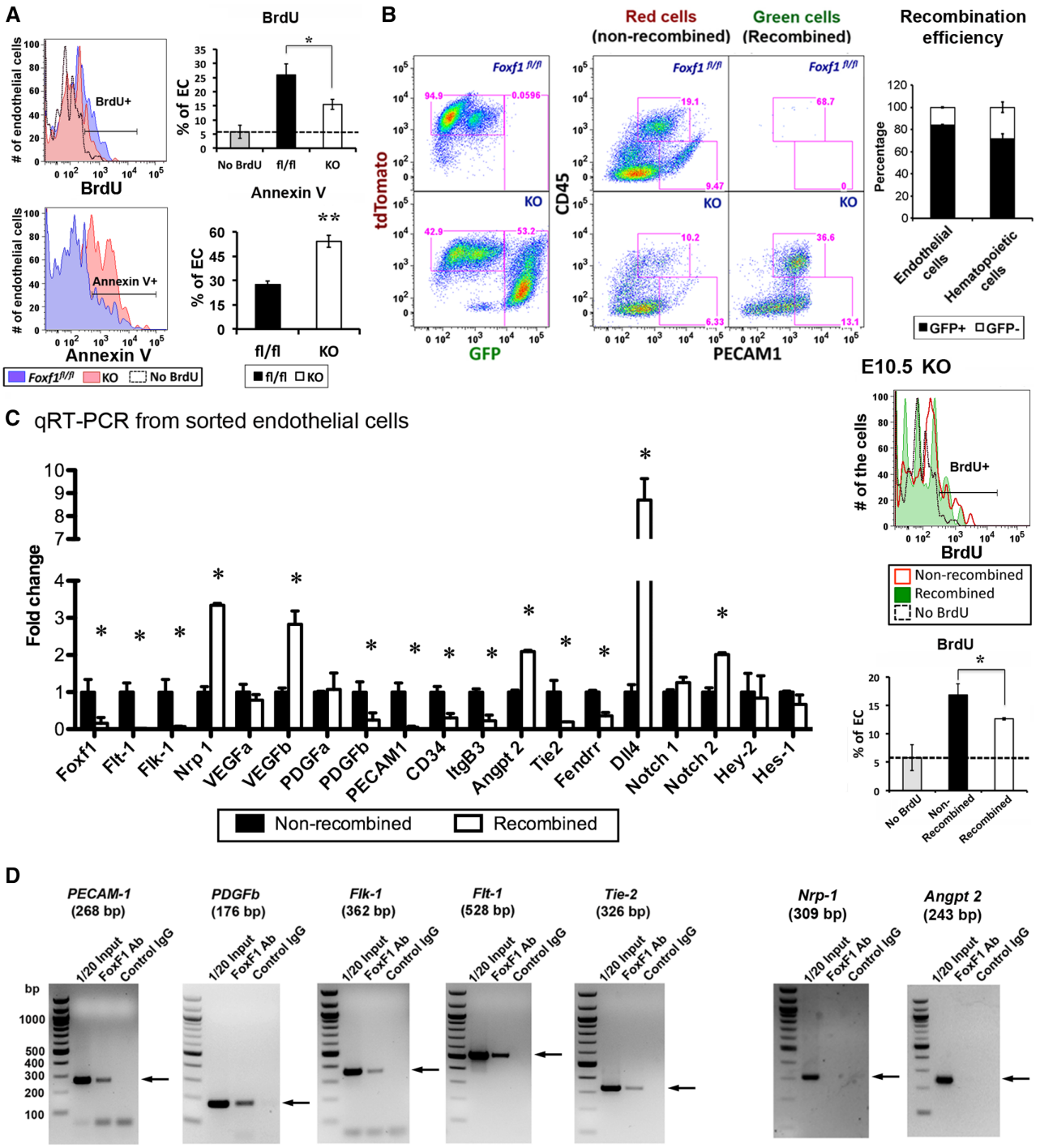

Figure 7. Forkhead Box transcription factor F1 (FOXF1) directly regulates expression of endothelial genes critical for angiogenesis and vascular endothelial growth factor signaling. A, Reduced BrdU incorporation and increased annexin V staining is detected by flow cytometry in endothelial cells of *Tie2-Cre Foxf1*$^{fl/fl}$ E12.5 embryos. The dotted line represents nonspecific staining with BrdU Abs. **B**, GFP and tdTomato fluorescence were measured in endothelial ($CD45^{-}PECAM\text{-}1^{+}$) and hematopoietic cells ($CD45^{+}PECAM\text{-}1^{-}$) isolated from *Tie2-Cre Foxf1*$^{fl/fl}$ *mT/mG* yolk sacs. GFP is not detected in cells from control *Foxf1*$^{fl/fl}$ *mT/mG* yolk sacs. Efficiency of Cre-mediated recombination is shown as a percentage of GFP^{+} cells among total cells isolated from the yolk sac (n=5; **right**). BrdU incorporation is decreased in GFP^{+} endothelial cells at E10.5 (**right middle**). **C**, Endothelial cells were flow-sorted from E12.5 yolk sacs. Quantitative reverse transcriptase polymerase chain reaction was used to examine mRNAs. **D**, Chromatin immunoprecipitation (ChIP) assay shows that FOXF1 binds to promoter regions of *Pecam-1*, *Pdgfb*, *Tie-2*, *Flt1*, and *Flk1* genes. FOXF1 does not bind to *Nrp1* and *Angpt2* promoters. Fetal endothelial MFLM-91U cells were used for ChIP. **P*<0.05, ***P*<0.01.

vascular insufficiency in FOXF1-deficient embryos. Previous studies demonstrated that *Foxc2* and *Foxc1* genes are critical for vascular development in zebrafish and mice.[5,32] We found no significant differences in expression of FOXC2 and FOXC1 after deletion of FOXF1. Because FOXC proteins and FOXF1 have high homology in their DNA-binding

domains, it is possible that FOXC1/2 can compensate for the loss of FOXF1 from endothelial cells by regulating similar target genes.

Published studies reported a direct correlation between FOXF1 levels and the number of pulmonary capillaries during lung development[14] and lung injury.[16] In the present study, we used in vivo and in vitro models to demonstrate that FOXF1 induces angiogenesis, endothelial proliferation, and VEGF signaling through transcriptional activation of VEGF receptors Flk1 and Flt1 (Figure 7). Reduction of Flk1 and Flt1 in FOXF1 mutants is consistent with the role of these genes in stimulating proliferation and differentiation of endothelial cells, leading to formation and maturation of blood vessels.[3,4] In addition to VEGF signaling, FOXF1 may influence other signaling pathways critical for endothelial development, such as PDGF and Angpt/Tie2 pathways. Reduced expression of Pdgfb and Tie2 may account for decreased proliferation and increased apoptosis of endothelial cells in FOXF1-deficient embryos. Our data also suggest that FOXF1 stimulates angiogenesis through transcriptional activation of *integrin-β3*, *pecam-1*, and lncRNA *Fendrr*, all of which are critical for vascular development.[5–7,33] Altogether, disruption of several key endothelial cell regulators can contribute to the FOXF1 phenotype. Because FOXF1 is a downstream target of the Shh signaling pathway,[15,18,19] it is possible that FOXF1 mediates cross-talk between the Shh and VEGF pathways during development of embryonic vasculature. Our results suggest that inability of FOXF1-deficient endothelial cells to respond to VEGF, PDGF, and Angpt/Tie2 signaling is a key mechanism in development of alveolar capillary dysplasia in ACD/MPV fetuses and infants harboring inactivating mutations in the FOXF1 gene locus.

Acknowledgments

We thank Y. Zhang for excellent technical assistance.

Sources of Funding

This work was supported by National Institutes of Health grants HL 84151 (to V.V. Kalinichenko) and CA 142724 (T.V. Kalin).

Disclosures

None.

References

1. Carmeliet P, Ferreira V, Breier G, Pollefeyt S, Kieckens L, Gertsenstein M, Fahrig M, Vandenhoeck A, Harpal K, Eberhardt C, Declercq C, Pawling J, Moons L, Collen D, Risau W, Nagy A. Abnormal blood vessel development and lethality in embryos lacking a single VEGF allele. *Nature*. 1996;380:435–439.
2. Ferrara N, Carver-Moore K, Chen H, Dowd M, Lu L, O'Shea KS, Powell-Braxton L, Hillan KJ, Moore MW. Heterozygous embryonic lethality induced by targeted inactivation of the VEGF gene. *Nature*. 1996;380:439–442.
3. Shalaby F, Rossant J, Yamaguchi TP, Gertsenstein M, Wu XF, Breitman ML, Schuh AC. Failure of blood-island formation and vasculogenesis in Flk-1-deficient mice. *Nature*. 1995;376:62–66.
4. Fong GH, Rossant J, Gertsenstein M, Breitman ML. Role of the Flt-1 receptor tyrosine kinase in regulating the assembly of vascular endothelium. *Nature*. 1995;376:66–70.
5. De Val S, Black BL. Transcriptional control of endothelial cell development. *Dev Cell*. 2009;16:180–195.
6. Arora R, Papaioannou VE. The murine allantois: a model system for the study of blood vessel formation. *Blood*. 2012;120:2562–2572.
7. Tiozzo C, Carraro G, Al Alam D, Baptista S, Danopoulos S, Li A, Lavarreda-Pearce M, Li C, De Langhe S, Chan B, Borok Z, Bellusci S, Minoo P. Mesodermal Pten inactivation leads to alveolar capillary dysplasia- like phenotype. *J Clin Invest*. 2012;122:3862–3872.
8. Bishop NB, Stankiewicz P, Steinhorn RH. Alveolar capillary dysplasia. *Am J Respir Crit Care Med*. 2011;184:172–179.
9. Stankiewicz P, Sen P, Bhatt SS, et al. Genomic and genic deletions of the FOX gene cluster on 16q24.1 and inactivating mutations of FOXF1 cause alveolar capillary dysplasia and other malformations. *Am J Hum Genet*. 2009;84:780–791.
10. Garabedian MJ, Wallerstein D, Medina N, Byrne J, Wallerstein RJ. Prenatal Diagnosis of Cystic Hygroma related to a Deletion of 16q24.1 with Haploinsufficiency of FOXF1 and FOXC2 Genes. *Case Rep Genet*. 2012;2012:490408.
11. Peterson RS, Lim L, Ye H, Zhou H, Overdier DG, Costa RH. The winged helix transcriptional activator HFH-8 is expressed in the mesoderm of the primitive streak stage of mouse embryos and its cellular derivatives. *Mech Dev*. 1997;69:53–69.
12. Kalinichenko VV, Zhou Y, Bhattacharyya D, Kim W, Shin B, Bambal K, Costa RH. Haploinsufficiency of the mouse Forkhead Box f1 gene causes defects in gall bladder development. *J Biol Chem*. 2002;277:12369–12374.
13. Mahlapuu M, Ormestad M, Enerbäck S, Carlsson P. The forkhead transcription factor Foxf1 is required for differentiation of extra-embryonic and lateral plate mesoderm. *Development*. 2001;128:155–166.
14. Kalinichenko VV, Lim L, Stolz DB, Shin B, Rausa FM, Clark J, Whitsett JA, Watkins SC, Costa RH. Defects in pulmonary vasculature and perinatal lung hemorrhage in mice heterozygous null for the Forkhead Box f1 transcription factor. *Dev Biol*. 2001;235:489–506.
15. Mahlapuu M, Enerbäck S, Carlsson P. Haploinsufficiency of the forkhead gene Foxf1, a target for sonic hedgehog signaling, causes lung and foregut malformations. *Development*. 2001;128:2397–2406.
16. Kalinichenko VV, Zhou Y, Shin B, Stolz DB, Watkins SC, Whitsett JA, Costa RH. Wild-type levels of the mouse Forkhead Box f1 gene are essential for lung repair. *Am J Physiol Lung Cell Mol Physiol*. 2002;282:L1253–L1265.
17. Kalinichenko VV, Bhattacharyya D, Zhou Y, Gusarova GA, Kim W, Shin B, Costa RH. Foxf1 +/- mice exhibit defective stellate cell activation and abnormal liver regeneration following CCl4 injury. *Hepatology*. 2003;37:107–117.
18. Madison BB, McKenna LB, Dolson D, Epstein DJ, Kaestner KH. FoxF1 and FoxL1 link hedgehog signaling and the control of epithelial proliferation in the developing stomach and intestine. *J Biol Chem*. 2009;284:5936–5944.
19. Szafranski P, Dharmadhikari AV, Brosens E, et al. Small noncoding differentially methylated copy-number variants, including lncRNA genes, cause a lethal lung developmental disorder. *Genome Res*. 2013;23:23–33.
20. Malin D, Kim IM, Boetticher E, Kalin TV, Ramakrishna S, Meliton L, Ustiyan V, Zhu X, Kalinichenko VV. Forkhead box F1 is essential for migration of mesenchymal cells and directly induces integrin-beta3 expression. *Mol Cell Biol*. 2007;27:2486–2498.
21. Kalinichenko VV, Gusarova GA, Kim IM, Shin B, Yoder HM, Clark J, Sapozhnikov AM, Whitsett JA, Costa RH. Foxf1 haploinsufficiency reduces Notch-2 signaling during mouse lung development. *Am J Physiol Lung Cell Mol Physiol*. 2004;286:L521–L530.
22. Claxton S, Kostourou V, Jadeja S, Chambon P, Hodivala-Dilke K, Fruttiger M. Efficient, inducible Cre-recombinase activation in vascular endothelium. *Genesis*. 2008;46:74–80.
23. Sandell LL, Iulianella A, Melton KR, Lynn M, Walker M, Inman KE, Bhatt S, Leroux-Berger M, Crawford M, Jones NC, Dennis JF, Trainor PA. A phenotype-driven ENU mutagenesis screen identifies novel alleles with functional roles in early mouse craniofacial development. *Genesis*. 2011;49:342–359.
24. Kalin TV, Wang IC, Meliton L, Zhang Y, Wert SE, Ren X, Snyder J, Bell SM, Graf L Jr, Whitsett JA, Kalinichenko VV. Forkhead Box m1 transcription factor is required for perinatal lung function. *Proc Natl Acad Sci U S A*. 2008;105:19330–19335.
25. Wang IC, Snyder J, Zhang Y, Lander J, Nakafuku Y, Lin J, Chen G, Kalin TV, Whitsett JA, Kalinichenko VV. Foxm1 mediates cross talk between Kras/mitogen-activated protein kinase and canonical Wnt pathways during development of respiratory epithelium. *Mol Cell Biol*. 2012;32:3838–3850.
26. Kalin TV, Meliton L, Meliton AY, Zhu X, Whitsett JA, Kalinichenko VV. Pulmonary mastocytosis and enhanced lung inflammation in mice heterozygous null for the Foxf1 gene. *Am J Respir Cell Mol Biol*. 2008;39:390–399.

27. Ren X, Shah TA, Ustiyan V, Zhang Y, Shinn J, Chen G, Whitsett JA, Kalin TV, Kalinichenko VV. FOXM1 promotes allergen-induced goblet cell metaplasia and pulmonary inflammation. *Mol Cell Biol*. 2013;33:371–386.
28. Wang IC, Zhang Y, Snyder J, Sutherland MJ, Burhans MS, Shannon JM, Park HJ, Whitsett JA, Kalinichenko VV. Increased expression of FoxM1 transcription factor in respiratory epithelium inhibits lung sacculation and causes Clara cell hyperplasia. *Dev Biol*. 2010;347:301–314.
29. Ustiyan V, Wang IC, Ren X, Zhang Y, Snyder J, Xu Y, Wert SE, Lessard JL, Kalin TV, Kalinichenko VV. Forkhead box M1 transcriptional factor is required for smooth muscle cells during embryonic development of blood vessels and esophagus. *Dev Biol*. 2009;336:266–279.
30. Ren X, Zhang Y, Snyder J, Cross ER, Shah TA, Kalin TV, Kalinichenko VV. Forkhead box M1 transcription factor is required for macrophage recruitment during liver repair. *Mol Cell Biol*. 2010;30:5381–5393.
31. Suri C, Jones PF, Patan S, Bartunkova S, Maisonpierre PC, Davis S, Sato TN, Yancopoulos GD. Requisite role of angiopoietin-1, a ligand for the TIE2 receptor, during embryonic angiogenesis. *Cell*. 1996;87:1171–1180.
32. De Val S, Chi NC, Meadows SM, Minovitsky S, Anderson JP, Harris IS, Ehlers ML, Agarwal P, Visel A, Xu SM, Pennacchio LA, Dubchak I, Krieg PA, Stainier DY, Black BL. Combinatorial regulation of endothelial gene expression by ets and forkhead transcription factors. *Cell*. 2008;135:1053–1064.
33. Grote P, Wittler L, Hendrix D, Koch F, Währisch S, Beisaw A, Macura K, Bläss G, Kellis M, Werber M, Herrmann BG. The tissue-specific lncRNA Fendrr is an essential regulator of heart and body wall development in the mouse. *Dev Cell*. 2013;24:206–214.
34. Kalinichenko VV, Lim L, Shin B, Costa RH. Differential expression of forkhead box transcription factors following butylated hydroxytoluene lung injury. *Am J Physiol Lung Cell Mol Physiol*. 2001;280:L695–L704.

Novelty and Significance

What Is Known?

- Inactivating mutations in the Forkhead Box transcription factor F1 (*FOXF1*) gene are found in 40% of patients with alveolar capillary dysplasia with misalignment of pulmonary veins.
- Haploinsufficiency of the *Foxf1* gene causes alveolar capillary dysplasia and developmental defects in lung, intestinal, and gall bladder morphogenesis in mice.
- FOXF1 is a transcription factor, which is found in multiple cell types, including endothelial cells.

What New Information Does This Article Contribute?

- Disruption of *Foxf1* gene in endothelial cells caused embryonic lethality, growth retardation, and cardiovascular abnormalities.
- Disruption of *Foxf1* reduced cell proliferation, increased apoptosis, and inhibited the vascular endothelial growth factor (VEGF) signaling pathway in endothelial cells.
- FOXF1 induces transcription of VEGF receptor genes *Flk1* and *Flt1*.

Inactivating mutations in the *FOXF1* gene were recently found in 40% of human patients with alveolar capillary dysplasia with misalignment of pulmonary veins. The molecular mechanisms by which these mutations cause vascular defects remain unknown. In the present study, we used transgenic mice with endothelial-specific inactivation of the *Foxf1* gene to demonstrate that FOXF1 is critical for formation of embryonic vasculature. FOXF1 stimulates endothelial proliferation and promotes the VEGF signaling pathway in embryonic endothelial cells through direct transcriptional activation of VEGF receptor genes. Our results suggest that inability of FOXF1-deficient endothelial cells to respond to VEGF signaling is a key mechanism in development of alveolar capillary dysplasia in alveolar capillary dysplasia with misalignment of pulmonary veins fetuses and infants harboring inactivating mutations in the *FOXF1* gene. Pharmacological agents that stimulate or stabilize FOXF1 protein might serve as promising therapeutic agents in patients with alveolar capillary dysplasia with misalignment of pulmonary veins caused by heterozygous loss-of-function mutations in *FOXF1* gene.

SUPPLEMENTAL MATERIAL

Detailed Methods

Mice. *Tie2-Cre* transgenic mice were purchased from Jackson Lab., whereas *Pdgfb-CreER* transgenic mice were obtained from Pierre Chambon [1]. *Flk1-null* mutant mice were previously described [2]. The *LoxP-stop-LoxP-βgal* (R26R) and the *LoxP-tdTomato-LoxP-GFP* (*mT/mG*) reporter mouse lines were from Jackson Lab. The *Foxf1*$^{fl/fl}$ mouse line was generated in the Kalinichenko lab (Cincinnati Children's Hospital Medical Center). *Foxf1*-targeting vector contained a LoxP site inserted into the *Foxf1* promoter and PGK-gb2 LoxP/FRT-flanked Neomycin (neo) cassette placed into the first intron. The PGK promoter-driven herpes simplex virus-thymidine kinase (HSV-TK) gene was placed outside of the *Foxf1* gene homology region for negative selection of non-homologous recombination in ES cells. The *Foxf1*^{fl}-targeting vector was used for electroporation of mouse ES cells (C57Bl/6 x 129/SVEV mouse background), which were selected for neo (G418) and HSV-TK resistance (ganciclovir) at the inGenious Targeting Laboratory (Stony Brook, NY). ES cells with the appropriate *Foxf1*^{fl}-targeted locus were identified by PCR and Southern blot analysis and were used to generate chimeric mice by injecting *Foxf1*^{fl} ES cells into mouse blastocysts. Mice containing the *Foxf1*^{fl}-targeted allele were determined by PCR amplification with primers flanking the LoxP sequence located in the *Foxf1* promoter and primers located in the 3' region of the *Foxf1*^{fl} allele. Primer sequences are provided in Suppl. Table. S1. To produce *Foxf1*$^{fl/+}$ mice, chimeric mice were bred with C57Bl/6 mice in the animal facility of Cincinnati Children's Hospital Medical Center. The Neo cassette was deleted by breeding of *Foxf1*$^{fl/+}$ mice with ACT-FLP1 mice (Jackson Lab.). The loss of Neo in *Foxf1*$^{fl/+}$ mice was confirmed by PCR using primers described in Suppl. Table. S1. *Foxf1*$^{fl/+}$ mice were backcrossed to generate viable *Foxf1*$^{fl/fl}$ mice that were bred into the C57Bl/6 background for ten generations. Deletion of the *Foxf1*^{fl} alleles from endothelial and hematopoietic cell lineages was accomplished through breeding with *Tie2-Cre* and *Pdgfb-CreER* transgenic mice. Deletion of FOXF1 was confirmed by breeding FOXF1-deficient mice with *LoxP-stop-LoxP-βgal* (R26R) and *LoxP-tdTomato-LoxP-GFP* (*mT/mG*) reporter mice. Animal studies were approved by the Animal Care and Use Committee of Cincinnati Children's Hospital Research Foundation.

RNA preparation and quantitative real-time RT-PCR (qRT-PCR). Total RNA was prepared from cultured MFLM-91U cells, mouse tissue and flow-sorted endothelial cells using RNeasy micro kit from Qiagen (Germantown, MD). qRT-PCR analysis was performed using a StepOnePlus Real-Time PCR system (Applied Biosystems, Foster City, CA) as described [3]. Samples were amplified using inventoried TaqMan primers for the gene of interest as indicated in Online Table II. Reactions were analyzed in triplicates and expression levels were normalized to β-actin mRNA. Five embryos were used in each group.

siRNA transfection, Western blot and matrigel angiogenesis assay. MFLM-91U cells were cultured in serum-free UltraCULTURE medium (Lonza, Walkersville, MD). To inhibit FOXF1, we transfected siRNA specific to mouse *Foxf1* (siFoxf1, 5′ -GAA AGG AGU UUG UCU UCU C-3', Dharmacon) using Lipofectamine™ 2000 reagent (Invitrogen) as described [4, 5]. Controls included mock-transfected cells and cells transfected with control non-targeting siRNA (Dharmacon). Cells were harvested 48 hours after transfection and used for matrigel angiogenesis assay (BD Biosciences). VEGF 165 (20 ng/ml, Millipore) was added to matrigel for 14 hr. Cells in matrigel were stained with calcein AM fluorescent viability dye which is transported through the cellular membrane into live cells. 3D images were acquired using a Nikon Eclipse Ti confocal microscope in conjunction with NIS-Elements AR software. Vessel filament total length and circularity were measured using IMARIS software (Bitplane, CT).

Western Blot analysis was performed using following antibodies: Foxf1 [4], Pecam-1 (ABCAM, Cat# ab28364-100), Flk1 (Santa Cruz, Cat# SC-6251), Flt1 (R&D, Cat# AF471), Pdgfb, (Aviva Systems Biology, Cat# ARP58509), Angpt2 (Rockland, Cat# 100-401-402), p-ERK 1/2 (Cell signaling, clone D13.14.4E), total ERK 1/2 (Cell signaling, clone 137F5), p-Akt (Cell signaling, clone 736E11), total Akt

(Cell signaling, clone 11E7) and β-actin (Sigma, clone AC-15). Detection of the immune complex was accomplished by using secondary antibodies directly conjugated with HRP followed by the Supersignal chemiluminescence substrate (Pierce, Rockford, IL).

Immunohistochemical staining and Flow cytometry. Paraffin sections were stained with hematoxylin and eosin (H&E) or used for immunohistochemical staining as described [6, 7]. The following antibodies were used for immunohistochemistry: FOXF1 [4], Pecam-1 (ABCAM, Cat# ab28364-100), Sox-17 (generated in Dr. Whitsett lab), Flk1 (Cell signaling, Cat# 55B11), LYVE-1 (Novas biologicals, Cat# NB100-725), Ephrin B2 (R&D systems, Cat# AF496) and endomucin (R&D systems, Cat#AF4666). Antibody-antigen complexes were detected using biotinylated secondary antibody followed by avidin-horseradish peroxidase (HRP) complex and DAB substrate (Vector Labs, Burlingame, CA). Sections were counterstained with nuclear fast red. To stain endothelial cells, Alexa Fluor 488-conjugated Isolectin B4 (Invitrogen) was used according to manufacturer recommendations and previous studies [8]. For co-localization experiments, secondary antibodies conjugated with Alexa Fluor 488 or Alexa Fluor 594 (Invitrogen) were used. Slides were counterstained with DAPI (Vector Lab). Fluorescent images were obtained using a Zeiss Axioplan2 microscope equipped with an AxioCam MRm digital camera and AxioVision 4.3 Software (Carl Zeiss Microimaging, Thornwood, NY).

Flow cytometry was performed using cells isolated from yolk sacs and lungs as described [7, 9]. Cells were stained with fluorescently-labeled antibodies against CD45 (eBioscience, clone 30-F11), CD41 (eBioscience, clone eBioMWReg30), Tie2 (eBioscience, clone TEK4), endomucin (eBioscience, clone eBioV.7C7), Pecam-1 (eBioscience, clone 390) or BrdU (eBioscience, clone BU20A). BrdU-labeling reagent (Invitrogen) was injected i.p. into pregnant females 2 hr prior to embryo harvest. Apoptosis was measured using the Annexin V kit (eBioscience). Cells stained with fixed viability dye, CD45 and Pecam-1 Abs were separated using cell sorting (Five-laser FACSAria II, BD Biosciences). Purified cells were used for RNA preparation and qRT-PCR analysis.

Chromatin Immunoprecipitation (ChIP) assay. ChIP assay was performed with *in situ* cross-linked MFLM-91U cells as described [3, 7]. Nuclear extracts from MFLM-91U cells were cross-linked by addition of formaldehyde, sonicated and used for the immunoprecipitation with Abs against FOXF1 [4] or control rabbit IgG (Vector Lab). DNA fragments were 500-700 bp. Reverse cross-linked ChIP DNA samples were subjected to PCR using the oligonucleotides specific to promoter regions of potential FOXF1-target genes. Sense (S) and antisense (AS) PCR primers that were used to amplify mouse promoter DNA fragments in ChIP assay are provided in Online Table III.

Statistical analysis. ANOVA and Student's T-test was used to determine statistical significance. P values less then 0.05 were considered significant. Values for all measurements were expressed as the mean ± standard deviation (SD).

Online Figure Legends

Online Fig. I. Genomic sequences of *Foxf1-floxed* and *Foxf1* wild type alleles. The first LoxP site was inserted into the promoter region of *Foxf1* gene. Primer P1 and P2 were used for genotyping. The second LoxP site is located in the intron of the *Foxf1* gene. The Neo sequence located in *Foxf1-floxed* allele was excised through Flp1-Frt recombination. Open box shows sequences that were deleted in *Tie2-Cre Foxf1$^{fl/fl}$* endothelial cells. Deleted sequences include part of the *Foxf1* promoter (977 bp), the first exon (white letters on gray background), Frt sequence and 62 bp of the intron. Identity of DNA sequence is denoted with *.

Online Fig. II. Ventricular hypoplasia and interventricular septum defect in *Tie2-Cre Foxf1$^{fl/fl}$* embryos. (A-B) *Tie2-Cre Foxf1$^{fl/fl}$* embryos were harvested at E12.5, E13.5 and E14.5. Transverse paraffin sections of thoracic region were stained with H&E. *Tie2-Cre Foxf1$^{fl/fl}$* embryos exhibited ventricular hypoplasia and the interventricular septum defect (asterisk in A). Decreased thickness of the left ventricular wall is observed in *Tie2-Cre Foxf1$^{fl/fl}$* embryos (black arrowheads in B). (C) H&E staining shows normal heart structure in *Tie2-Cre Foxf1$^{fl/fl}$* E10.5 embryos. Abbreviations: RA, right atrium; LA, left atrium; RV, right ventricle; LV, left ventricle; ES, esophagus; DAo, dorsal aorta. Scale bars are 50 μm.

Online Fig. III. Vascular abnormalities in *Tie2-Cre Foxf1$^{fl/fl}$*, *Foxf1$^{+/-}$* and *Flk1-null* embryos. (A) Diminished branching of blood vessels is observed in placenta of *Tie2-Cre Foxf1$^{fl/fl}$* E13.5 embryos (KO) compared to control *Foxf1$^{fl/fl}$* littermates (fl/fl). (B-C) Vascular abnormalities in *Foxf1$^{+/-}$* embryos. *Foxf1$^{+/-}$* E12.5 embryos exhibit polyhydramnios (white arrowheads in left B panel). Wild type littermates (WT) are shown for comparison. PCR of genomic tail DNA identifies the *Foxf1-null* and *Foxf1 WT* alleles (middle panel in B). Western blot shows reduced FOXF1 protein in lung tissue obtained from *Foxf1$^{+/-}$* embryos (right panel in B). Diminished vascular branching in the yolk sac of *Foxf1$^{+/-}$* E12.5 embryos (C). The whole mount immunoistaining of the yolk sac was performed using endomucin Abs (upper panel in C). Confocal microscopy was used to quantitate vessel density by calculating a ratio between endomucin^{+} endothelial area and E-cadherin^{+} epithelial area (bottom panel in C). $p<0.05$ is *. (D) *Flk1-null* embryos show growth retardation at E10.5. Endomucin staining shows the lack of blood vessels in *Flk1-null* yolk sacs. Scale bars are 200 μm.

Online Fig. IV. Expression of arterial, venous and lymphatic markers in *Tie2-Cre Foxf1$^{fl/fl}$* embryos. (A) Paraffin sections from *Tie2-Cre Foxf1$^{fl/fl}$* (KO) and control *Foxf1$^{fl/fl}$* E12.5 embryos were stained for LYVE1 and Ephrin B2. Slides were counterstained with nuclear fast red (red nuclei). Ephrin B2 staining was decreased in endothelial cells of aorta. Lymphatic vessels (LYVE1^{+}) were not altered after FOXF1 deletion. LYVE1 staining (dark brown) is shown with arrowheads. The images were taken from transverse sections of thoracic region. (B) Total RNA was prepared from either yolk sacs (left panel) or purified yolk sac endothelial cells (right panel) of *Tie2-Cre Foxf1$^{fl/fl}$* (KO) and control *Foxf1$^{fl/fl}$* E12.5 embryos and analyzed by qRT-PCR. Decreased ephrin B2 mRNA was found in *Tie2-Cre Foxf1$^{fl/fl}$* yolk sacs ($p<0.05$ is *). *Ephrin B4, Sox-18, Foxc1 and Foxc2* mRNAs were not significantly altered (n=5). Expression levels were normalized to β-actin mRNA. Abbreviations: DA, dorsal aorta; Es, esophagus; Br, bronchus; Sk, skin. Scale bars are 20 μm.

Online Fig. V. Flow cytometry for hematopoietic and endothelial markers in *Tie2-Cre Foxf1$^{fl/fl}$* E10.5 yolk sacs. (A-B) Cells purified from E10.5 yolk sacs were used for flow cytometry. Hematopoietic cells were subdivided on CD45^{+} (mature) and CD45^{lo}CD41^{+} (immature) subsets. There was no difference in the number of either CD45^{+} or CD45^{lo}CD41^{+} cells in Tie2-Cre Foxf1$^{fl/fl}$ E10.5 yolk sacs (A). Endothelial cells were identified as CD45^{-}PECAM-1^{+} cells that also expressed Tie2 and endomucin (EDCN). The number of endothelial cells was significantly decreased in Tie2-Cre Foxf1$^{fl/fl}$ E10.5 yolk

sacs compared to controls (B). $p<0.05$ is *, $p<0.01$ is **. (C) Immunostaining shows that FOXF1 is expressed in atrioventricular cardiac cushion (CC) and endothelial cells of placenta and yolk sac. FOXF1 is not expressed in hematopoietic cells located within blood vessels. Scale bars are 20μm.

Online Fig. VI. Reduced angiogenesis in retina of *Pdgfb-CreER Foxf1*$^{fl/fl}$ mice. (A) *Pdgfb-CreER Foxf1*$^{fl/fl}$ newborns were treated with tamoxifen at P0, P1 and P2. Mice were harvested at P6.5. (B-C) Retinal blood vessels were visualized using whole mount staining for isolectin B4. Red arrow shows retinal vascular outgrowth from the optic stalk. White arrowheads indicate endothelial sprouts at angiogenic front. Decreased retinal vasculature outgrowth is found in tamoxifen-treated *Pdgfb-CreER Foxf1*$^{fl/fl}$ mice (n=5) compared to *Foxf1*$^{fl/fl}$ controls (n=6). $p<0.05$ is indicated with * (C). Scale bars: B, upper panels, 300μm; B, lower panels, 100μm.

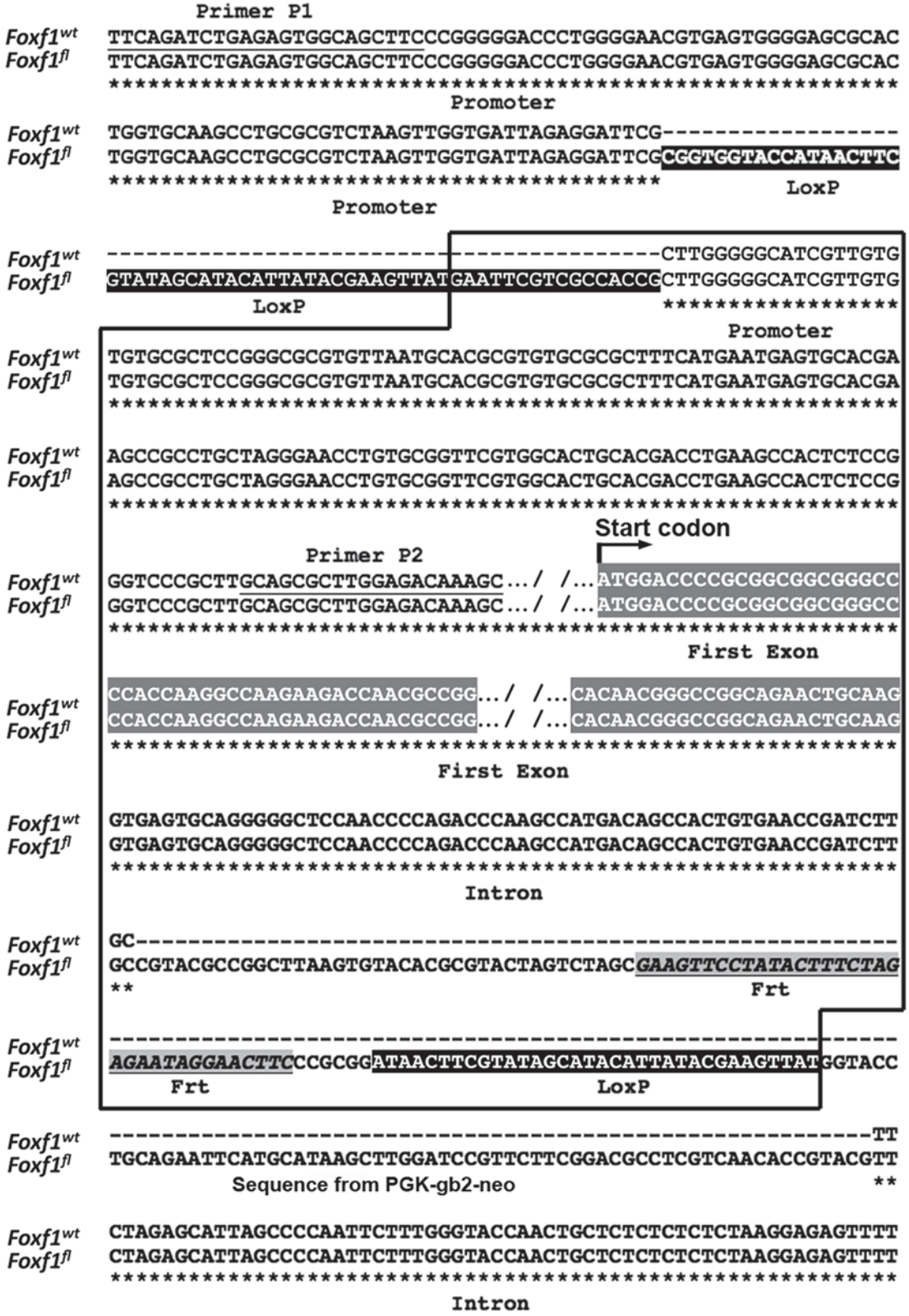

Online Fig. I. Genomic sequences of *Foxf1-floxed* and *Foxf1* wild type alleles. The first LoxP site was inserted into the promoter region of *Foxf1* gene. Primer P1 and P2 were used for genotyping. The second LoxP site is located in the intron of the *Foxf1* gene. The Neo sequence located in *Foxf1-floxed* allele was excised through Flp1-Frt recombination. Open box shows sequences that were deleted in *Tie2-Cre Foxf1*$^{fl/fl}$ endothelial cells. Deleted sequences include part of the *Foxf1* promoter (977 bp), the first exon (white letters on gray background), Frt sequence and 62 bp of the intron. Identity of DNA sequence is denoted with *.

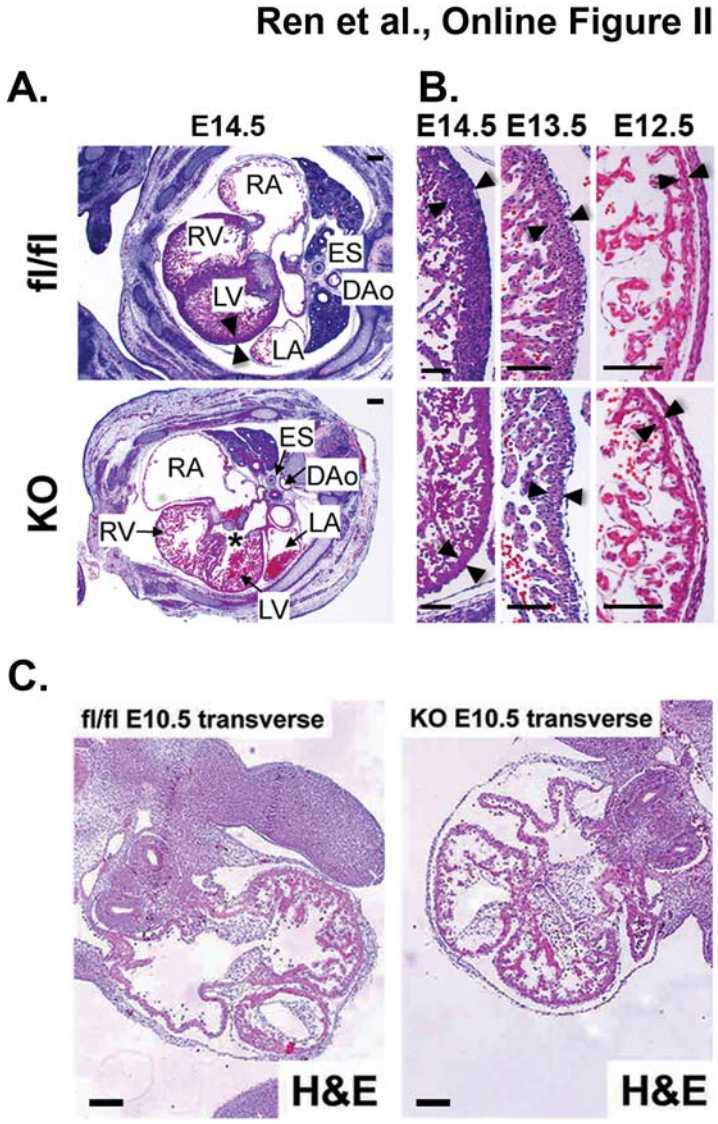

Online Fig. II. Ventricular hypoplasia and interventricular septum defect in *Tie2-Cre Foxf1*$^{fl/fl}$ embryos. (A-B) *Tie2-Cre Foxf1*$^{fl/fl}$ embryos were harvested at E12.5, E13.5 and E14.5. Transverse paraffin sections of thoracic region were stained with H&E. *Tie2-Cre Foxf1*$^{fl/fl}$ embryos exhibited ventricular hypoplasia and the interventricular septum defect (asterisk in A). Decreased thickness of the left ventricular wall is observed in *Tie2-Cre Foxf1*$^{fl/fl}$ embryos (black arrowheads in B). (C) H&E staining shows normal heart structure in *Tie2-Cre Foxf1*$^{fl/fl}$ E10.5 embryos. Abbreviations: RA, right atrium; LA, left atrium; RV, right ventricle; LV, left ventricle; ES, esophagus; DAo, dorsal aorta. Scale bars are 50 μm.

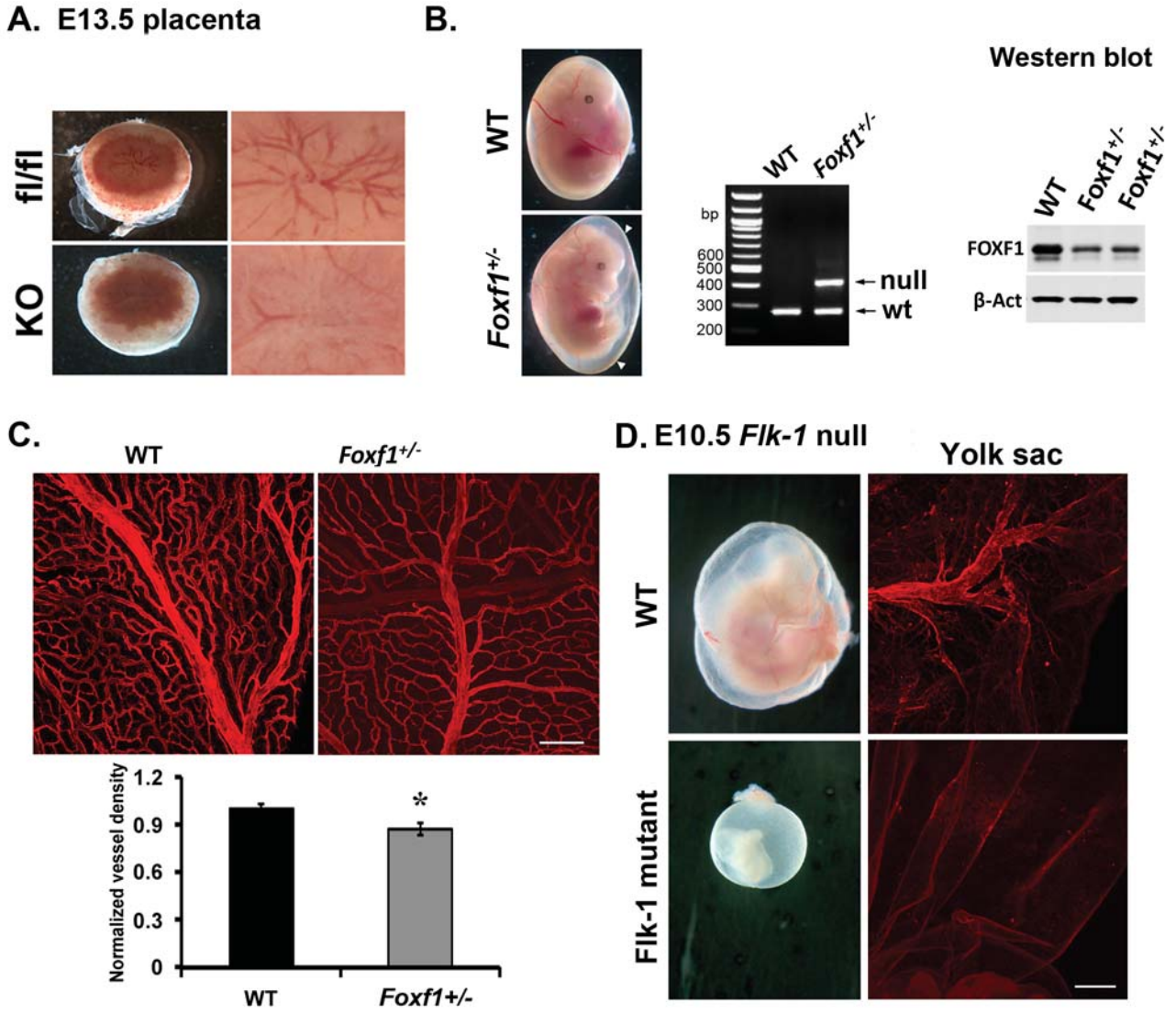

Online Fig. III. Vascular abnormalities in *Tie2-Cre Foxf1$^{fl/fl}$*, *Foxf1$^{+/-}$* and *Flk1-null* embryos. (A) Diminished branching of blood vessels is observed in placenta of *Tie2-Cre Foxf1$^{fl/fl}$* E13.5 embryos (KO) compared to control *Foxf1$^{fl/fl}$* littermates (fl/fl). (B-C) Vascular abnormalities in *Foxf1$^{+/-}$* embryos. *Foxf1$^{+/-}$* E12.5 embryos exhibit polyhydramnios (white arrowheads in left B panel). Wild type littermates (WT) are shown for comparison. PCR of genomic tail DNA identifies the *Foxf1-null* and *Foxf1 WT* alleles (middle panel in B). Western blot shows reduced FOXF1 protein in lung tissue obtained from *Foxf1$^{+/-}$* embryos (right panel in B). Diminished vascular branching in the yolk sac of *Foxf1$^{+/-}$* E12.5 embryos (C). The whole mount immunoistaining of the yolk sac was performed using endomucin Abs (upper panel in C). Confocal microscopy was used to quantitate vessel density by calculating a ratio between endomucin^{+} endothelial area and E-cadherin^{+} epithelial area (bottom panel in C). $p<0.05$ is *. (D) *Flk1-null* embryos show growth retardation at E10.5. Endomucin staining shows the lack of blood vessels in *Flk1-null* yolk sacs. Scale bars are 200 μm.

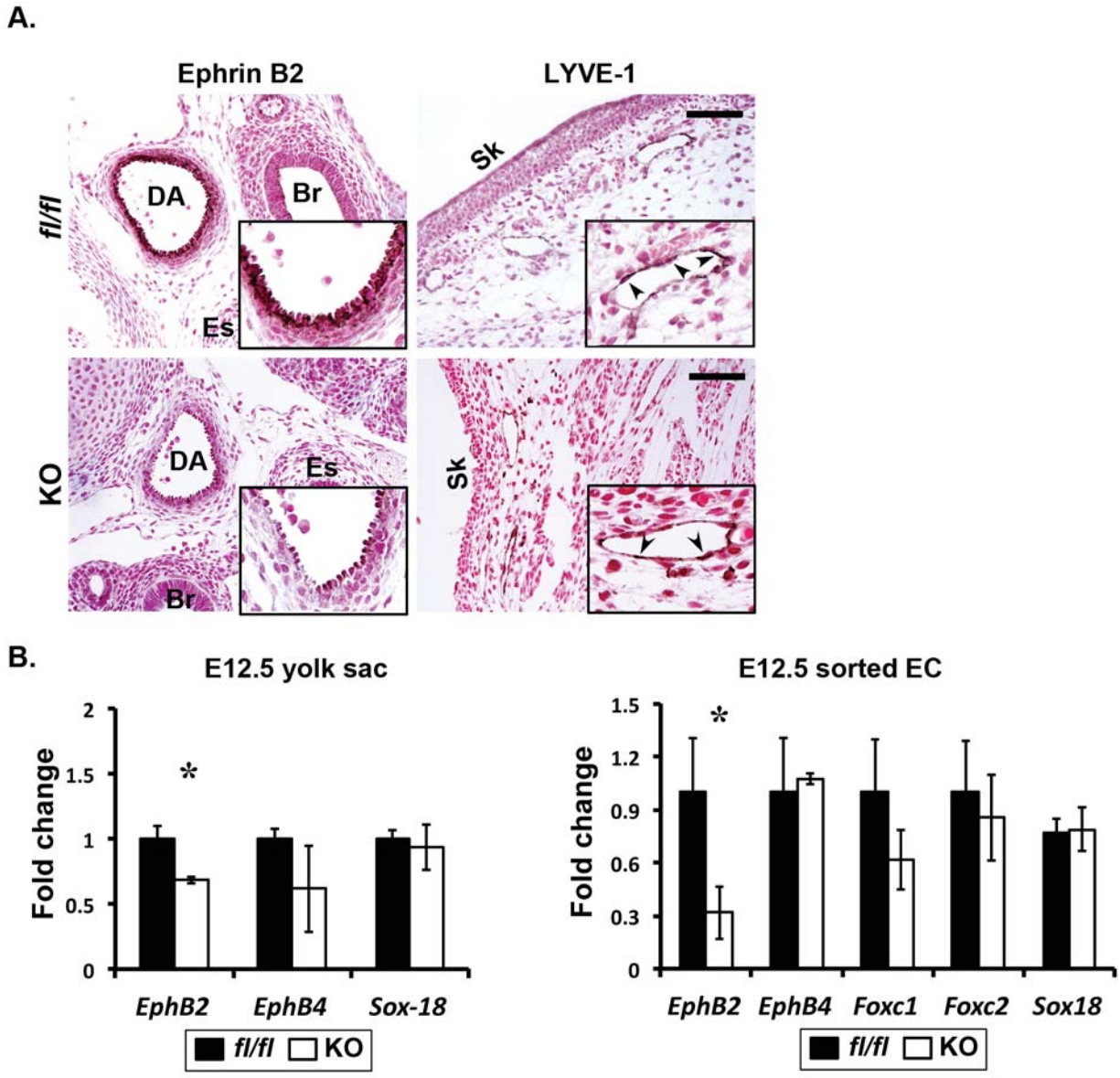

Online Fig. IV. Expression of arterial, venous and lymphatic markers in *Tie2-Cre Foxf1$^{fl/fl}$* embryos
(A) Paraffin sections from *Tie2-Cre Foxf1$^{fl/fl}$* (KO) and control *Foxf1$^{fl/fl}$* E12.5 embryos were stained for LYVE1 and Ephrin B2. Slides were counterstained with nuclear fast red (red nuclei). Ephrin B2 staining was decreased in endothelial cells of aorta. Lymphatic vessels (LYVE1^{+}) were not altered after FOXF1 deletion. LYVE1 staining (dark brown) is shown with arrowheads. The images were taken from transverse sections of thoracic region. (B) Total RNA was prepared from either yolk sacs (left panel) or purified yolk sac endothelial cells (right panel) of *Tie2-Cre Foxf1$^{fl/fl}$* (KO) and control *Foxf1$^{fl/fl}$* E12.5 embryos and analyzed by qRT-PCR. Decreased ephrin B2 mRNA was found in *Tie2-Cre Foxf1$^{fl/fl}$* yolk sacs ($p<0.05$ is *). *Ephrin B4, Sox-18, Foxc1 and Foxc2* mRNAs were not significantly altered (n=5). Expression levels were normalized to β-actin mRNA. Abbreviations: DA, dorsal aorta; Es, esophagus; Br bronchus; Sk, skin. Scale bars are 20 μm.

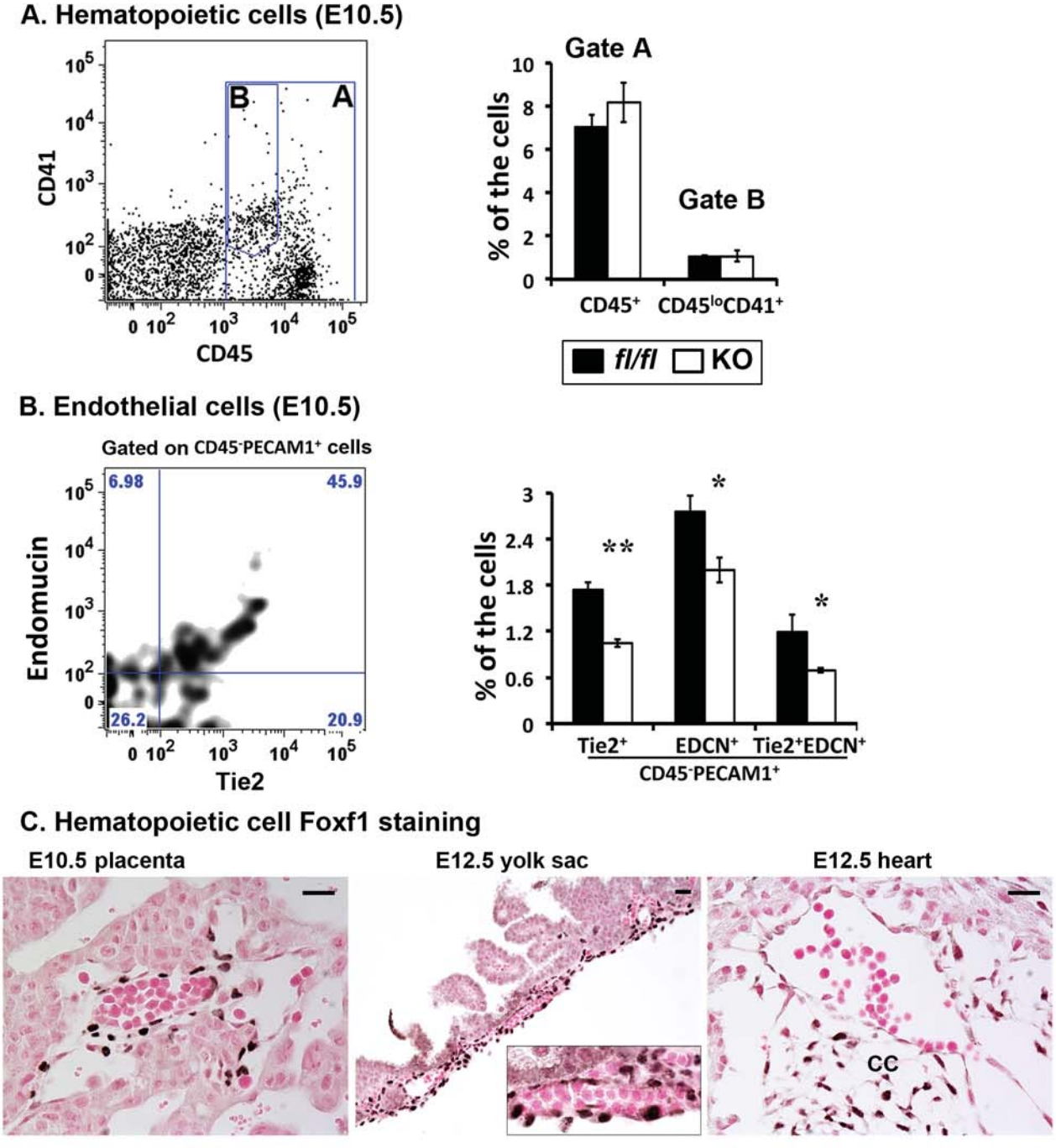

Online Fig. V. Flow cytometry for hematopoietic and endothelial markers in *Tie2-Cre Foxf1$^{fl/fl}$* E10.5 yolk sacs. (A-B) Cells purified from E10.5 yolk sacs were used for flow cytometry. Hematopoietic cells were subdivided on CD45^{+} (mature) and CD45^{lo}CD41^{+} (immature) subsets. There was no difference in the number of either CD45^{+} or CD45^{lo}CD41^{+} cells in Tie2-Cre Foxf1$^{fl/fl}$ E10.5 yolk sacs (A). Endothelial cells were identified as CD45^{-}PECAM-1^{+} cells that also expressed Tie2 and endomucin (EDCN). The number of endothelial cells was significantly decreased in Tie2-Cre Foxf1$^{fl/fl}$ E10.5 yolk sacs compared to controls (B). $p<0.05$ is *, $p<0.01$ is **. (C) Immunostaining shows that FOXF1 is expressed in atrioventricular cardiac cushion (CC) and endothelial cells of placenta and yolk sac. FOXF1 is not expressed in hematopoietic cells located within blood vessels. Scale bars are 20μm.

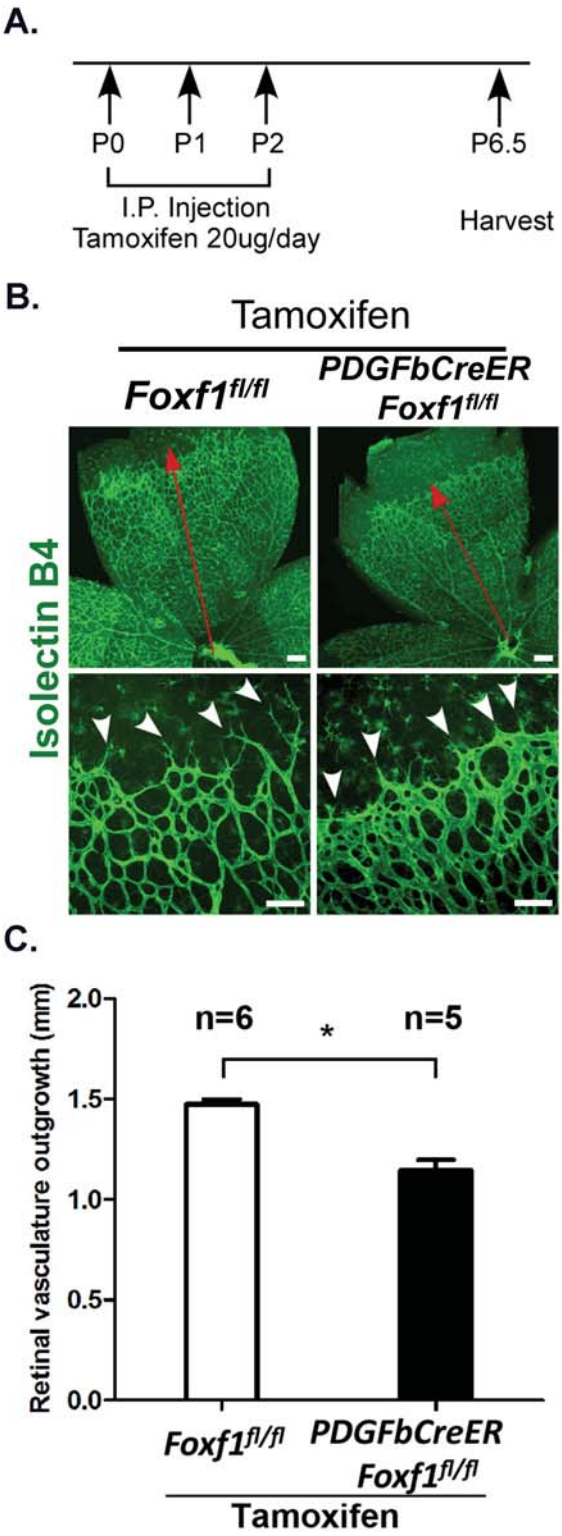

Online Fig. VI. Reduced angiogenesis in retina of *Pdgfb-CreER Foxf1*$^{fl/fl}$ mice. (A) *Pdgfb-CreER Foxf1*$^{fl/fl}$ newborns were treated with tamoxifen at P0, P1 and P2. Mice were harvested at P6.5. (B-C) Retinal blood vessels were visualized using whole mount staining for isolectin B4. Red arrow shows retinal vascular outgrowth from the optic stalk. White arrowheads indicate endothelial sprouts at angiogenic front. Decreased retinal vasculature outgrowth is found in tamoxifen-treated *Pdgfb-CreER Foxf1*$^{fl/fl}$ mice (n=5) compared to *Foxf1*$^{fl/fl}$ controls (n=6). $p<0.05$ is indicated with * (C). Scale bars: B, upper panels, 300μm; B, lower panels, 100μm.

Online Tables

Online Table I. Primers for genotyping

Primer name	Sequence
P1	5'-*TTCAGATCTGAGAGTGGCAGCTTC*-3'
P2	5'-*GCTTTGTCTCCAAGCGCTGC*-3'
P3	5'-*CCAGAGGCCACTTGTGTAGC*-3'
P4	5'-*TAATACTGAGAGGGCAGAGCTACGTG*-3'
P5	5'-*CTCCCTGGAGCAGCCATACC*-3'
P6	5'-*GCTCCTGCCGAGAAAGTATCC*-3'
P7	5′-*GAAGGAACCCAGATGTTCCCTG*-3′

Online Table II. TaqMan primers for qRT-PCR reactions

Mouse TaqMan gene expression assay	Catalog No.
Foxf1	Mm00487497_m1
Beta-actin	Mm00607939_s1
Pecam1	Mm01242584_m1
Sox-17	Mm00488363_m1
Flk-1	Mm01222421_m1
Flt-1	Mm00438980_m1
Cd34	Mm00519283_m1
Nrp1	Mm00435379_m1
Pdgfa	Mm01205760_m1
Pdgfb	Mm01298578_m1
Vegfa	Mm00437304_m1
Vegfb	Mm00442102_m1
Angpt1	Mm00456503_m1
Angpt2	Mm00549822_m1
Itgb3	Mm00443980_m1
Tie2	Mm01256892_m1
Fendrr	Mm01248996_m1
Ephb2	Mm01215897_m1
Ephb4	Mm01201157_m1
Dll4	Mm00444619_m1
Notch1	Mm00435249_m1
Notch2	Mm00803077_m1
Hey2	Mm00469280_m1
Hes1	Mm00468601_m1
Foxc1	Mm01962704_s1
Foxc2	Mm00546194_s1
Sox18	Mm00656049_gH

Online Table III. Primers for ChIP assay

Primer Name	Sequence
Pecam1 Sense	*5′-CTTAACACCTTAGCAACTAGAGCTC-3′*
Pecam1 Anti-sense	*5′-ATGGCAAGATGCCTTTGAACACAAC-3′*
Pdgfb Sense	*5′-TAGATGAGTTCTGGGACTGGACT-3′*
Pdgfb Anti-sense	*5′-AGACATAACCGGAGGAGAAGAAG-3′*
Flk1 Sense	*5′-TGTATTAGAGGAGACACTGTCTTC-3′*
Flk1 Anti-sense	*5′-CGTATGAAGGCTGCTTGGTGTAC-3′*
Flt1 Sense	*5′-CTTAGCTACTTCAATTACGAGGC-3′*
Flt1 Anti-sense	*5′-AAGGACTATCCTAACGCCCAC-3′*
Tie2 Sense	*5′-GCTCCTGTAGACATAATCACTTCTG-3′*
Tie2 Anti-sense	*5′-TGCTCTACAGCTTAGGCAAGCCT-3′*
Nrp1 Sense 1	*5′-CAGTTCTCTAAGATCAACAGCGTG-3′*
Nrp1 Anti-sense 1	*5′-TAGTCTACCTTGACGAGATCTCTG-3′*
Nrp1 Sense 2	*5′-TCTTGATGGGATCCTATGGCACAG-3′*
Nrp1 Anti-sense 2	*5′-CTATTGTTTCTCATTTTCCAGAACTGAGG-3′*
Angpt2 Sense 1	*5′-AACCAAATACCAACAAGACTTTACTTC-3′*
Angpt2 Anti-sense 1	*5′-CGTTTGTAGGCTAAGCTTGC-3′*
Angpt2 Sense 2	*5′-TTAAAGTGATTACCTCAGATACTCTGC-3′*
Angpt2 Anti-sense 2	*5′-GCTCACCCACTATCTTCCTGT-3′*

Supplemental References

1. Claxton S, Kostourou V, Jadeja S, Chambon P, Hodivala-Dilke K, Fruttiger M. Efficient, inducible Cre-recombinase activation in vascular endothelium. *Genesis.* 2008;46:74-80.

2. Sandell LL, Iulianella A, Melton KR, Lynn M, Walker M, Inman KE, Bhatt S, Leroux-Berger M, Crawford M, Jones NC, Dennis JF, Trainor PA. A phenotype-driven ENU mutagenesis screen identifies novel alleles with functional roles in early mouse craniofacial development. *Genesis.* 2011;49:342-359.

3. Kalin TV, Wang IC, Meliton L, Zhang Y, Wert SE, Ren X, Snyder J, Bell SM, Graf L, Jr., Whitsett JA, Kalinichenko VV. Forkhead Box m1 transcription factor is required for perinatal lung function. *Proceedings of the National Academy of Sciences of the United States of America.* 2008;105:19330-19335.

4. Malin D, Kim IM, Boetticher E, Kalin TV, Ramakrishna S, Meliton L, Ustiyan V, Zhu X, Kalinichenko VV. Forkhead box F1 is essential for migration of mesenchymal cells and directly induces integrin-beta3 expression. *Molecular and cellular biology.* 2007;27:2486-2498.

5. Wang IC, Snyder J, Zhang Y, Lander J, Nakafuku Y, Lin J, Chen G, Kalin TV, Whitsett JA, Kalinichenko VV. Foxm1 Mediates Cross Talk between Kras/Mitogen-Activated Protein Kinase and Canonical Wnt Pathways during Development of Respiratory Epithelium. *Molecular and cellular biology.* 2012;32:3838-3850.

6. Kalin TV, Meliton L, Meliton AY, Zhu X, Whitsett JA, Kalinichenko VV. Pulmonary mastocytosis and enhanced lung inflammation in mice heterozygous null for the Foxf1 gene. *American journal of respiratory cell and molecular biology.* 2008;39:390-399.

7. Ren X, Shah TA, Ustiyan V, Zhang Y, Shinn J, Chen G, Whitsett JA, Kalin TV, Kalinichenko VV. FOXM1 promotes allergen-induced goblet cell metaplasia and pulmonary inflammation. *Molecular and cellular biology.* 2013;33:371-386.

8. Kalinichenko VV, Lim L, Beer-Stoltz D, Shin B, Rausa FM, Clark J, Whitsett JA, Watkins SC, Costa RH. Defects in Pulmonary Vasculature and Perinatal Lung Hemorrhage in Mice Heterozygous Null for the Forkhead Box f1 transcription factor. *Developmental biology.* 2001;235:489-506.

9. Ren X, Zhang Y, Snyder J, Cross ER, Shah TA, Kalin TV, Kalinichenko VV. Forkhead box M1 transcription factor is required for macrophage recruitment during liver repair. *Molecular and cellular biology.* 2010;30:5381-5393.

Circulation Research
JOURNAL OF THE AMERICAN HEART ASSOCIATION

FOXF1 Transcription Factor Is Required for Formation of Embryonic Vasculature by Regulating VEGF Signaling in Endothelial Cells

Xiaomeng Ren, Vladimir Ustiyan, Arun Pradhan, Yuqi Cai, Jamie A. Havrilak, Craig S. Bolte, John M. Shannon, Tanya V. Kalin and Vladimir V. Kalinichenko

Circ Res. 2014;115:709-720; originally published online August 4, 2014;
doi: 10.1161/CIRCRESAHA.115.304382
Circulation Research is published by the American Heart Association, 7272 Greenville Avenue, Dallas, TX 75231

Print ISSN: 0009-7330. Online ISSN: 1524-4571